AWARD NUMBER: W81XWH-14-1-0318

TITLE: Genetic and Diagnostic Biomarker Development in ASD Toddlers Using Resting State Functional MRI

PRINCIPAL INVESTIGATOR: Glahn, David C.

CONTRACTING ORGANIZATION: Yale University
                                        New Haven, CT 06511

REPORT DATE: November 2017

TYPE OF REPORT: Final

PREPARED FOR: U.S. Army Medical Research and Materiel Command
                            Fort Detrick, Maryland 21702-5012

DISTRIBUTION STATEMENT: Approved for Public Release;
                                        Distribution Unlimited

The views, opinions and/or findings contained in this report are those of the author(s) and should not be construed as an official Department of the Army position, policy or decision unless so designated by other documentation.

REPORT DOCUMENTATION PAGE		*Form Approved* *OMB No. 0704-0188*

Public reporting burden for this collection of information is estimated to average 1 hour per response, including the time for reviewing instructions, searching existing data sources, gathering and maintaining the data needed, and completing and reviewing this collection of information. Send comments regarding this burden estimate or any other aspect of this collection of information, including suggestions for reducing this burden to Department of Defense, Washington Headquarters Services, Directorate for Information Operations and Reports (0704-0188), 1215 Jefferson Davis Highway, Suite 1204, Arlington, VA 22202-4302. Respondents should be aware that notwithstanding any other provision of law, no person shall be subject to any penalty for failing to comply with a collection of information if it does not display a currently valid OMB control number. **PLEASE DO NOT RETURN YOUR FORM TO THE ABOVE ADDRESS.**

1. REPORT DATE	2. REPORT TYPE	3. DATES COVERED
November 2017	Final	1 Sep 2014 - 31 Aug 2017

4. TITLE AND SUBTITLE	5a. CONTRACT NUMBER
Genetic and Diagnostic Biomarker Development in ASD Toddlers Using Resting State Functional MRI	
	5b. GRANT NUMBER
	W81XWH-14-1-0318
	5c. PROGRAM ELEMENT NUMBER

6. AUTHOR(S)	5d. PROJECT NUMBER
Glahn, David C	
	5e. TASK NUMBER
	5f. WORK UNIT NUMBER
E-Mail: david.glahn@yale.com	

7. PERFORMING ORGANIZATION NAME(S) AND ADDRESS(ES)	8. PERFORMING ORGANIZATION REPORT NUMBER
New Haven, CT 06511 Yale University	

9. SPONSORING / MONITORING AGENCY NAME(S) AND ADDRESS(ES)	10. SPONSOR/MONITOR'S ACRONYM(S)
U.S. Army Medical Research and Materiel Command Fort Detrick, Maryland 21702-5012	
	11. SPONSOR/MONITOR'S REPORT NUMBER(S)

12. DISTRIBUTION / AVAILABILITY STATEMENT

Approved for Public Release; Distribution Unlimited

13. SUPPLEMENTARY NOTES

14. ABSTRACT

Our overarching strategy is to exploit three large neuroimaging/neurobehavioral datasets to identify brain-imaging based biomarkers for Autism Spectrum Disorders (ASD). At Yale, we focus on determining if brain networks are influenced by genetic factors and if these genetic factors also influence other traits associated with ASD. Specifically, we will provide heritability estimates and test for pleitropy between putative ASD functional and structural networks and cognitive and behavioral traits. Further, we examined the impact of non-synonymous protein coding genetic variants on these ASD connectivity traits.

15. SUBJECT TERMS

Autism spectrum disorder (ASD); biomarker; early brain development; intrinsic functional brain networks; hertitability; genetic control; pleitropy

16. SECURITY CLASSIFICATION OF:			17. LIMITATION OF ABSTRACT	18. NUMBER OF PAGES	19a. NAME OF RESPONSIBLE PERSON USAMRMC
a. REPORT	b. ABSTRACT	c. THIS PAGE			19b. TELEPHONE NUMBER *(include area code)*
Unclassified	Unclassified	Unclassified	Unclassified	40	

Standard Form 298 (Rev. 8-98)
Prescribed by ANSI Std. Z39.18

TABLE OF CONTENTS

Page

1. INTRODUCTION

Our strategy is to exploit three large neuroimaging/neurobehavioral datasets in order to identify brain-imaging based biomarkers for Autism Spectrum Disorders (ASD), including 1) BrainMap, developed and maintained by Peter Fox at the University of Texas Health Science Center at San Antonio (UTHSCSA); 2) the Autism Center of Excellence (ACE) neuroimaging archive, developed and maintained by Eric Courchesne at the University of California at San Diego (UCSD); and 3) the Genetics of Brain Structure (GOBS) neuroimaging genetics archive, developed and maintained by David Glahn at Yale University. To develop ASD biomarkers, we aim to (1) develop multi-regional functional-connectivity models of networks implicated in ASD by iterative and hierarchical meta-analyses of the BrainMap database; (2) test the ability of the neural-system functional-connectivity models to differentiate between ASD and TYP children in a cohort previously acquired ACE cohort; and assess the heritability and pleitropy of the these functional networks, in a previously imaged and previously genotyped cohort of families with extended pedigrees. At Yale, we focus on the final aim, estimating heritability of putative ASD networks and testing for pleitropy between these networks and cognitive and behavioral measures.

Given delays associated with generating whole genome sequence data on the GOBS cohort, we requested and received a 1 year no cost extension.

2. KEYWORDS

Autism spectrum disorder (ASD); biomarker; early brain development; intrinsic functional brain networks; functional MRI (fMRI); clinical outcome; genomic; heritability; genetic control; pleitropy

3. ACCOMPLISHMENTS

a. What were the major goals of the Yale site?

At the Yale site, we focus estimating heritability of putative ASD functional and structural networks, testing for pleitropy between these networks and cognitive and behavioral measures and training post-doctoral associates and others to conduct the needed analyses. Below we outline the major tasks identified in the original Scope of Work (SOW) relevant for this reporting period.

Administrative Tasks (Prior to Aims)

Major Task 1 *was to submit and obtain ethics approval from our local ethical review board*. We accomplished this goal (Milestone #1) ahead of schedule: Yale's Human Research Protection Program board approved the project on April 15, 2014 (HIC 1403013622).

Major Task 2 *was to advertise, interview, hire and train staff dedicated for the project*. After several rounds of interviews and advertising in national and international scientific meetings, we offered a post-doctor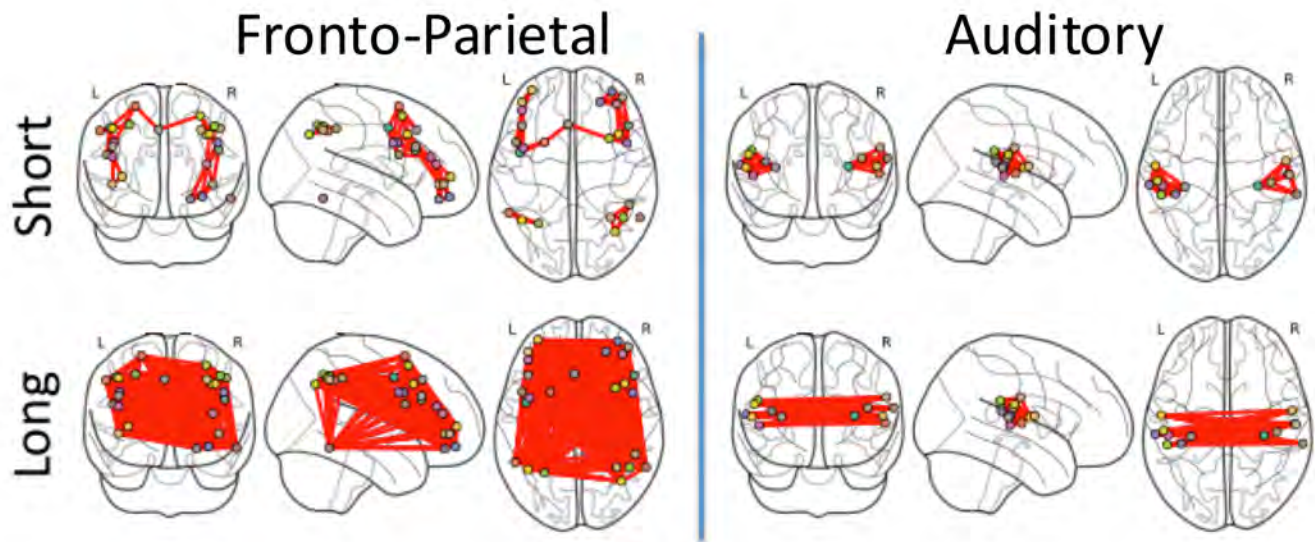al fellowship to Dr. Karen Hodgson (see section 7. **Participants**, below). Dr. Hodgson accepted the offer and joined our group in February of 2015. Dr. Hodgson was 100% dedicated to this project as a Postdoctoral Associate at Yale University, Department of Psychiatry, from February 1, 2015 to December 15, 2016. Dr. Hodgson underwent an extensive training program and has mastered the methods necessary for the genetic analyses to be conducted for this project (Milestone #2). She is currently an associate research scientist at King's College London.

Tasks In support of Specific Aim 3 (Yale University Site)

Major Task 1 *involved the pre-processing of structural and functional data for subjects from the GOBS cohort.* Pre-processing involved a number of quality control and analytic steps.

Quality control, preprocessing and neuroanatomic parcellation were performed on ~1500 scans from individuals in randomly ascertained extended pedigrees by April/May of 2015 (Subtask 1). In total, 1004 images were found to be of adequate quality and were reliably parcellated using FreeSurfer 5.1. Similarly, quality control, preprocessing and functional parcellation was conducted on ~900 scans from individuals in randomly ascertained extended pedigrees by May of 2015 (Subtask 2). In total, 783 images were found to be of adequate quality and were reliably parcellated into functional networks using ICA tools. Thus, Milestone #1 was accomplished for the GOBS cohort by May of 2015.
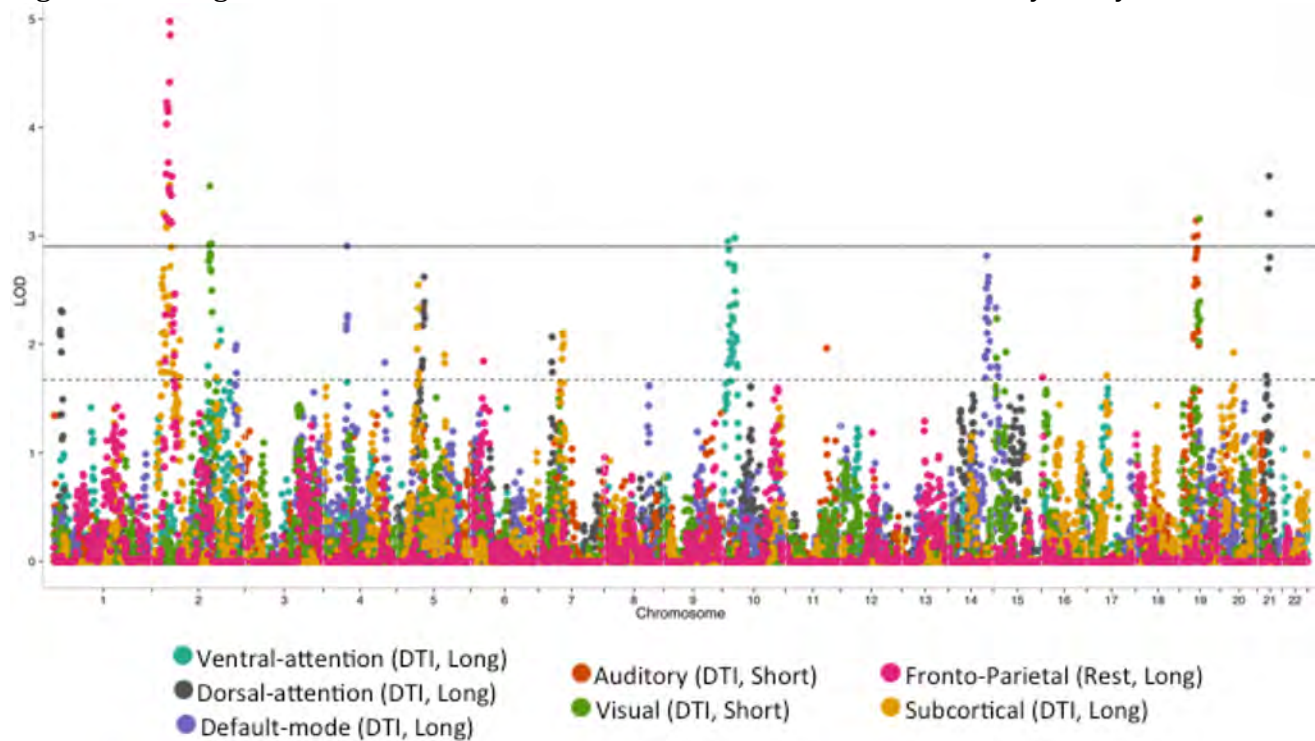
Figure 1. Example Functional Connectivity Networks based upon methods by Power et al (2013)

Major Task 2 *involved conducting intrinsic connectivity analyses from functional networks derived from the BrainMap and ACE datasets.* Two "agnostic" intrinsic connectivity analyses were conducted by August of 2015. The first, utilized an extension of the methods initially published by Power and colleagues (Power JD, Schlaggar BL, Lessov-Schlaggar CN, Petersen SE. Evidence for hubs in human functional brain networks. Neuron. 2013 Aug 21;79(4):798-813. PMID: 23972601). This approach uses over 250 seed regions simultaneously to provide regional and network-level measures of brain connectivity. Using this analytic approach, we estimated heritability for a set of structural and functional networks, examined the co-heritability between these different modalities and searched the genome for chromosomal loci influencing these networks. In **Figure 1**, we provide examples of two of the 14 derived networks, based on the network configuration determined in the Power et al., work. For our current experiment, we defined network connections as either short or long (greater or less than 40mm). In **Figure 2**, we indicate the number and chromosomal locations of loci that influenced network-based connectivity measures found to be significantly heritable. Findings from these analyses were presented at the 21st annual meeting of the Organization for Human Brain Mapping in Honolulu, HI, entitled "Shared and Unique Genetic Influences on Structural and Functional Connectivity."

The second analytic approach involved the application of surface based analytic techniques developed by the Human Connectome Project (http://www.humanconnectome.org), a NIH roadmap initiative designed to map normal variation in brain connectivity. This computationally demanding analytic strategy derives dense connectivity maps for each subject based upon a surfaced based parelation and then combined these connectivity maps using a combined function-structure alignment strategy. This method provides similar heritability estimates as those derived using the Power et al method.

Figure 2. Linkage-Manhattan Plot for Structural and Functional Connectivity Analyses

After a prolong QC process, we searched the complete exome of ∼900 subjects for rare functional variants influencing the fronto-parietal and auditory networks. Unfortunately, no single variant reached statistical significance in this analysis. While this result is disappointing, our findings are consistent with other comparably powered exome sequencing studies. For example, analyses in a sample of ∼2500 trio ASD families (e.g. affected child and both parents) demonstrated that *de novo* loss of function mutations, often coalescing in gene-networks influencing chromatin modifiers, targets of fragile X mental retardation proteins (FMRP) and embryonically expressed genes, are strongly associated with risk for autism spectrum disorder (Iossifov et al., *Neuron*, 2012, PMID= 22542183; Sanders et al., *Nature*, 2012, PMID= 22495306). Based upon the overall mutation rates, current estimates suggest that between 400 and 1000 genes confer risk for autism spectrum disorder and that these genes appear to coalesce into gene networks influencing chromatin modification, synaptic function, targets of FMRP, targets of RBFOX splicing factors, and early embryonic development (Iossifov et al., *Neuron*, 2012, PMID= 22542183; Sanders et al., *Nature*, 2012, PMID= 22495306; De Rubeis et al. *Nature* 2014, PMID= 25363760; Iossifov et al., *Nature* 2014; PMID: 25363768). Yet, despite this progress, no signle
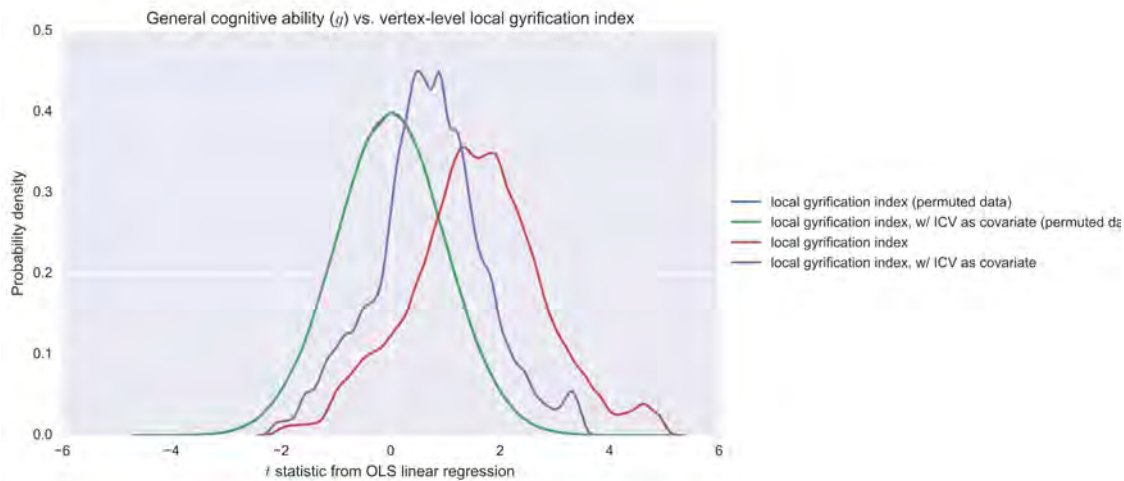
4

variant (or gene) has been defenitivly identified. This pattern of results is completely consistent with recent fidnings in schizophrenia. Using whoe exome sequence data, Purcell and colleagues (Purcell et al., Nature, 2014, PMID= 24463508) identified numerous rare mutations across many genes, that when considered in aggregate are strongly associated with schizophrenia risk, in 2,536 schizophrenia cases and 2,543 controls, and appear to be in networks that directly influence neuronal function, including the voltage-gated calcium ion channel, the activity-regulated cytoskeleton-associated scaffold protein (ARC), and the N-methyl-D-aspartate receptor (NMDAR) postsynaptic signaling complex. Many of these gene sets were previously implicated in schizophrenia risk through CNV analyses (Kirov et al., *Mol Psychiatry*, 2012, PMID= 22083728). Furthermore, based on exome data from 623 schizophrenia trios, *de novo* mutations are over represented among glutamatergic postsynaptic proteins comprising the ARC and NMDAR complexes in affected individuals (Fromer et al., *Nature*, 2014, PMID= 24463507), strikingly consistent with the much larger case-control results. Similarly, exome sequencing studies in schizophrenia have implicated genes expressed in neurons (Genovese et al., *Nat Neurosci,* 2016; PMID= 27694994) and synapses (Fromer et al., *Nature*, 2014, PMID= 24463507) and shown that affected individuals have more rare protein-altering loss-of-function variants than unrelated controls. However, definitive evidence for specific genes is still quite limited. Given these results and evidence for substantial polygenicity, the fields of autism and schizophrenia genetics have begun to focus on gene networks rather than one single gene effects. We too have begun using a similar approach and believe that our study is adequately powered to either identify a gene network associated with autism related dysconnectivity or to characterize a previously identified gene set. However, these analyses are outside of the scope of the current project.

In addition to the work with intrinsic connectivity traits described above, we have conducted a number of analyses relevant to brain-behavior changes in autism. For example, we recently examined the relationship between cortical gyrification and intelligence in our large, genetically informative population. Gyrification is the process of forming the characteristic folds of the human cerebral cortex and there are several articles indicating aberrant gyrification patterns in children and adults with autism (e.g. Wallace et al., *Brain*, 2013 PMID= 23715094; Hardan et al., *Psychiatry Res*, 2004 PMID= 15465295; Jou et al., J Child Neurol, 2010 PMID= 20413799). Furthermore, it appears that decreased gyrification in prefrontal cortex is associated with deficit functional connectivity in children with autism (Schaer et al., *Front Hum Neurosci*, 2013; PMID = 24265612). Finally, there is some evidence that gyrification patterns, particularly as they associate with IQ, may be an autism endophenotype, a trait sensitive to genetic liability for the illness (Kates et al., *Autism Res*, 2009 PMID= 19890876). Thus, examining the genetic influences the relationship between cortical gyrification and intelligence appears to be an interesting new way to dissect genetic liability for autism.

To date, our analyses have focused on replicating prior findings of the relationship between local gyrification patterns and intelligence (Gregory et al., Cur Biol, 2016 PMID=27133866). In two large cohorts, Gregory and colleagues found that general cognitive ability was significantly associated with increasing gyrification in a network of neocortical regions, including large portions of the prefrontal cortex, inferior parietal lobule, and temporoparietal junction, as well as the insula, cingulate cortex,

and fusiform gyrus. This pattern of results is consistent with the Parieto-Frontal Integration Theory of intelligence (Jung and Haier, *Behave Brain Sci*, 2007 PMID= 17655784) and with brain regions implicated in autism. Using data from 1004 individuals from the "Genetics of Brain Structure and Function" study, we generally replicate these findings. Further, we demonstrate that common genetic factors appear to influence local gyrification and a general cognitive ability index. Next, we plan to

Figure 3. Association between Local Gyrification and General Cognitive Ability (n~1000)

General cognitive ability (*g*) vs. vertex-level local gyrification index

Probability density

t statistic from OLS linear regression

— local gyrification index (permuted data)
— local gyrification index, w/ ICV as covariate (permuted data)
— local gyrification index
— local gyrification index, w/ ICV as covariate

determine the common genetic influences on gyrification/intelligence and risk for autism using a rare-variant based enrichment score developed in our laboratory. The goal of this analysis is to determine if genes (variants) associated with autism risk also influence the relationship between cortical gyrification and intelligence. If such a relationship can be established, then it is possible to enumerate some of the biological pathways through which risk genes give rise to autism risk. Such information is invaluable for the development of treatment or remediation strategies.

Finally, given evidence that both genetic and epigenetic factors appear to be important for autism risk (Persico & Bourgeron, 2006, *Trends Neurosci*, PMID: 16808981), we extended our project to examine epigenetic effects on white matter connectivity. White matter microstructure is reduced in individuals with autism spectrum disorders (Barnea-Goraly et al., *Biol Psychiatry*, 2004, PMID: 14744477) and appears to be related to developmental delays in language dysfunction (Herbert et al., 2004, *Ann Neurol*, PMID= 15048892). To determine if epigenetic influences on white matter microstructure (fractional anisotropy) as measured by diffusion tensor imaging, we conducted a set of experiments to model the impact or biological or epigenetic aging on MR-based white matter measurement in GOBS participants (Hodgson et al., *J Neurosci*, 2017, PMID= 28385874). The accurate estimation of age using methylation data has proved a useful and heritable biomarker, with acceleration in epigenetic age predicting a number of age-related phenotypes. Measures of white matter integrity in the brain are heritable and highly sensitive to both normal and pathological aging processes. We consider the phenotypic and genetic interrelationships between epigenetic age acceleration and white matter integrity in humans. Our goal was to investigate processes that underlie inter-individual variability in age-related changes in the brain. Using blood taken from a Mexican-American extended pedigree sample (n = 628; age = 23.28-93.11 years),

epigenetic age was estimated using the method developed by Horvath and colleagues (Horvath, *Genome Biol*, 2013, PMID= 24138928). For n = 376 individuals, diffusion tensor imaging scans were also available. The interrelationship between epigenetic age acceleration and global white matter integrity was investigated with variance decomposition methods. To test for neuroanatomical specificity, 16 specific tracts were additionally considered. We observed negative phenotypic correlations between epigenetic age acceleration and global white matter tract integrity (ρpheno = -0.119, p = 0.028), with evidence of shared genetic (ρgene = -0.463, p = 0.013) but not environmental influences. Negative phenotypic and genetic correlations with age acceleration were also seen for a number of specific white matter tracts, along with additional negative phenotypic correlations between granulocyte abundance and white matter integrity. These findings (i.e., increased acceleration in epigenetic age in peripheral blood correlates with reduced white matter integrity in the brain and shares common genetic influences) provide a window into the neurobiology of aging processes within the brain and a potential biomarker of normal and pathological brain aging. Our results were published in the *Journal of Neuroscience* earlier this year (Hodgson et al., *J Neurosci*, 2017, PMID= 28385874). Our goal is to apply this method to study white-matter abnormalities in autism spectrum disorders in the future.

These analyses fulfill Milestone #2.

b. What was accomplished under these goals at the Yale University site?

All of the work described above was conducted at the Yale site. In addition, a conceptually similar analysis was conducted using neuroanatomic networks disrupted in schizophrenia. Specifically, we used source-based morphometry, a multivariate technique optimized for structural MRI, in a large sample of randomly ascertained pedigrees (N = 887) to derive an insula-medial prefrontal cortex (mPFC) component and to investigate its genetic determinants. First, we replicated the insula-mPFC grey matter component as an independent source of grey matter variation in the general population, and verified its relevance to schizophrenia in an independent case-control sample. Secondly, we showed that the neuroanatomical variation defined by this component is largely determined by additive genetic variation (h^2 = 0.59), and genome-wide linkage analysis resulted in a significant linkage peak at 12q24 (*LOD* = 3.76). This region has been of significant interest to psychiatric genetics as it contains the Darier's disease locus and other proposed susceptibility genes (e.g. *DAO*, *NOS1*), and it has been linked to affective disorders and schizophrenia in multiple populations. Thus, in conjunction with previous clinical studies, our data imply that one or more psychiatric risk variants at 12q24 are co-inherited with reductions in mPFC and insula grey matter concentration. The results of these analyses were reported in a manuscript recently accepted for publication in a peer-reviewed journal. This article was published: Sprooten E, Gupta CN, Knowles EE, McKay DR, Mathias SR, Curran JE, Kent JW Jr, Carless MA, Almeida MA, Dyer TD, Göring HH, Olvera RL, Kochunov P, Fox PT, Duggirala R, Almasy L, Calhoun VD, Blangero J, Turner JA, Glahn DC. Genome-wide significant linkage of schizophrenia-related neuroanatomical trait to 12q24., Am J Med Genet B Neuropsychiatr Genet. 2015 Dec;168(8):678-86. PMID: 26440917. The success of this similar project speaks to the feasibility and potential for success of the ASD project.

c. What opportunities for training and professional development has the project provided at the Yale University site?

Although Dr. Karen Hodgson joined the team with considerable molecular genetics experience, she did not have formal training in quantitative or statistical genetics. Thus, in order for Dr. Hodgson to perform the analyses needed for the current project, she learned a new skill set involving the use of

complex analytic methods in the service of furthering our understanding of human brain connectivity in general and how connectivity is disrupted in ASD.

d. How were the results disseminated to communities of interest?

We have presented preliminary analyses at the 2015 annual meeting for the Organization for Human Brain Mapping. A manuscript describing a conceptually similar analysis was published in the American Journal of Medical Genetics Part B (2015). Finally, our epigenetic aging article appeared in the *Journal of Neuroscience* in 2017. These abstracts and paper appear in the appendices.

e. What do you plan to do during the next reporting period to accomplish the goals?

We have largely met the goals of our project. We clearly documented that functional connectivity alterations found in ASD is under genetic control. Although we were not able to definitively identify a gene for ASD connectivity deficits, this goal was an extension of our initial aims. Furthermore, our efforts to link autism related dysconnectivity to either empirically derived gene sets or to further characterize ASD related gene networks is ongoing. We are actively working to secure funding for these analyses.

4. IMPACT
a. What is the impact on understanding ASD brain development of the project?

As outlined above, we have a number of results that are directly relevant to the proposed project, further demonstrate the plausibility of the proposed analyses and improve our understanding of the neurogenetics of human brain connectivity.

b. What was the impact of the project results on other disciplines, technology transfer, or society beyond science and technology?

Other Disciplines: *Neurogenetics*. Thus far, our project has estimated the genetic control over functional and structural connectivity measures, documented that independent genetic factors appear to influence these traits, localized chromosomal loci influencing either functional, structural or both structural and functional connectivity, and demonstrated that epigenetic factors influence white matter coherence. These results are relevant for ASD, although work to create exact imaging biomarkers is ongoing.

Technology Transfer: Our initial findings were reported in an international scientific meeting in May 2015. A manuscript describing a conceptually similar analysis was published in the American Journal of Medical Genetics Part B (2015). Finally, our epigenetic aging article appeared in the *Journal of Neuroscience* in 2017. This abstract and papers appear in the appendices.

Society: Nothing to Report

5. CHANGES/PROBLEMS

No scientific, design, or experiment problems have occurred and thus no significant changes to the project are proposed. As described above, we completed pre-processing of functional and

structural connectivity measures using the originally proposed methods. However, newer surface-based methods developed by the Human Connectome Project have become available to the scientific community. Thus, we have implemented these methods as well and will conduct all analyses in parallel.

6. PRODUCTS

The products resulting from the project during the reporting period include the following conference paper:

- Glahn et al., "Shared and Unique Genetic Influences on Structural and Functional Connectivity," 21st annual meeting of the Organization for Human Brain Mapping, Honolulu, HI
- Sprooten E, Gupta CN, Knowles EE, McKay DR, Mathias SR, Curran JE, Kent JW Jr, Carless MA, Almeida MA, Dyer TD, Göring HH, Olvera RL, Kochunov P, Fox PT, Duggirala R, Almasy L, Calhoun VD, Blangero J, Turner JA, Glahn DC. Genome-wide significant linkage of schizophrenia-related neuroanatomical trait to 12q24., Am J Med Genet B Neuropsychiatr Genet. 2015 Dec;168(8):678-86. PMID: 26440917.
- Hodgson K, Carless MA, Kulkarni H, Curran JE, Sprooten E, Knowles EE, Mathias S, Göring HHH, Yao N, Olvera RL, Fox PT, Almasy L, Duggirala R, Blangero J, Glahn DC. Epigenetic Age Acceleration Assessed with Human White-Matter Images. J Neurosci. 2017 May 3;37(18):4735-4743. PMID: 28385874

7. PARTICIPANTS AND OTHER COLLABORATING ORGANIZATIONS

a. What individuals have worked on the project?

Work on this project has been limited to David C Glahn, PhD, the PD/PI, and Dr. Karen Hodgson, post-doctoral associate.

David C. Glahn, Ph.D. (0.6 calendar months), years 1-2. Partnering Principal Investigator is an expert in the application of neurocognitive and neuroimaging phenotypes in large-scale behavioral and molecular genetic studies of psychiatric illnesses. He is a Professor in the Department of Psychiatry, Yale University School of Medicine, and an Olin Neuropsychiatric Research Center Scholar where he directs the Imaging Genomics laboratory. As outlined in the Scope of Work, Dr. Glahn has ultimate responsibility for conducting neurocognitive, neuroimaging and behavioral genetic analyses in support of Specific Aim 3.

Karen Hodgson (7.2 calendar months, or 60% effort), years 1-2. Under the supervision of Dr. Glahn, this Dr. Hodgson has conduct neurocognitive, neuroimaging and behavioral genetic analyses in support of Specific Aim 3. In addition, she liaisons with other investigators involved in the project.

b. Has there been a change in the active other support of the PD/PI(s) or senior/key personnel since the last reporting period?

Nothing to Report

c. What other organizations were involved as partners?

As per the original application, the other organizations involved as partners are the University of Texas Health Science Center San Antonio (Dr. Fox, the overall project P.I.) and the University of California San Diego site (Dr. Courchesne, P.I. at that site).

8. SPECIAL REPORTING REQUIREMENTS

COLLABORATIVE AWARD: This project is part of a Collaborative Award and this Progress Report is from the Yale University site (Glahn). Comparable progress reports from Dr. Peter Fox at the University of Texas Health Science Center San Antonio and Dr. Eric Courchesne at University of California San Diego will be submitted separately.

9. APPENDICES

Attached is the published abstract for Glahn et al., "Shared and Unique Genetic Influences on Structural and Functional Connectivity," 21st annual meeting of the Organization for Human Brain Mapping, Honolulu, HI

Sprooten E, Gupta CN, Knowles EE, McKay DR, Mathias SR, Curran JE, Kent JW Jr, Carless MA, Almeida MA, Dyer TD, Göring HH, Olvera RL, Kochunov P, Fox PT, Duggirala R, Almasy L, Calhoun VD, Blangero J, Turner JA, Glahn DC. Genome-wide significant linkage of schizophrenia-related neuroanatomical trait to 12q24., Am J Med Genet B Neuropsychiatr Genet. 2015 Dec;168(8):678-86. PMID: 26440917 (pdf)

Hodgson K, Carless MA, Kulkarni H, Curran JE, Sprooten E, Knowles EE, Mathias S, Göring HHH, Yao N, Olvera RL, Fox PT, Almasy L, Duggirala R, Blangero J, Glahn DC. Epigenetic Age Acceleration Assessed with Human White-Matter Images. J Neurosci. 2017 May 3;37(18):4735-4743. PMID: 28385874 (pdf)

Glahn et al., "Shared and Unique Genetic Influences on Structural and Functional Connectivity," 21st annual meeting of the Organization for Human Brain Mapping, Honolulu, HI

Abstract: The relationship between in vivo measures of structural connectivity, often indexed with diffusion-weighted imagining, and functional connectivity, typically measured with resting-state functional MRI, appears to be complex. While structural connections appear to facilitate some aspects of functional connectivity, functional relationship may include multiple structural pathways. However, most systems neuroscience models of brain connectivity suggest that anatomical and physiological processes are dependent, in part, upon common neurobiological mechanisms. While there is growing evidence that measures of functional and structural connectivity are influenced by genetic factors, little is known about potential pleiotropy (e.g. the same genes influencing both structural and functional connectivity). Using 1606 individuals from extended pedigrees with both resting-state and diffusion weighted scans, we (1) establish the heritability of structural and functional connectivity in previously defined brain networks, (2) use genetic correlations to show statistical evidence that common genes influence both types of measures, and (3) show that specific chromosomal loci influence both structural and functional connectivity.

Genome-Wide Significant Linkage of Schizophrenia-Related Neuroanatomical Trait to 12q24

Emma Sprooten[1,2], Cota Navin Gupta[3], Emma EM Knowles[1,2], D Reese McKay[1,2], Samuel R Mathias[1,2], Joanne E Curran[4], Jack W Kent Jr[4], Melanie A Carless[4], Marcio A Almeida[4], Thomas D Dyer[4], Harald HH Göring[4], Rene L Olvera[5], Peter Kochunov[6], Peter T Fox[7], Ravi Duggirala[4], Laura Almasy[4], Vince D. Calhoun[1,3,8,10], John Blangero[4], Jessica A Turner[3,9], and **David C Glahn**[1,2]

[1]Department of Psychiatry, Yale University School of Medicine, New Haven, CT

[2]Olin Neuropsychiatry Research Center, Institute of Living, Hartford Hospital, CT

[3]The Mind Research Network, Albuquerque, NM

[4]Department of Genetics, Texas Biomedical Research Institute, San Antonio, TX

[5]Department of Psychiatry, University of Texas Health Science Center San Antonio, San Antonio, TX

[6]Maryland Psychiatric Research Center, Department of Psychiatry, University of Maryland School of Medicine, Baltimore, MD

[7]Research Imaging Institute, University of Texas Health Science Center San Antonio, San Antonio, TX

[8]Department of Psychiatry, University of New Mexico, Albuquerque, NM

[9]Department of Psychology and Neuroscience Institute, Georgia State University, Atlanta, GA

[10]Department of Electrical and Computer Engineering, University of New Mexico, Albuquerque, NM

Abstract

The insula and medial prefrontal cortex (mPFC) share functional, histological, transcriptional and developmental characteristics and they serve higher cognitive functions of theoretical relevance to schizophrenia and related disorders. Meta-analyses and multivariate analysis of structural magnetic resonance imaging (MRI) scans indicate that gray matter density and volume reductions in schizophrenia are the most consistent and pronounced in a network primarily composed of the insula and mPFC. We used source-based morphometry, a multivariate technique optimized for structural MRI, in a large sample of randomly ascertained pedigrees (N = 887) to derive an insula-mPFC component and to investigate its genetic determinants. Firstly, we replicated the insula-mPFC gray matter component as an independent source of gray matter variation in the general

Corresponding Author: Emma Sprooten Ph.D., Olin Neuropsychiatry Research Center, Whitehall Research Building, Institute of Living, 200 Retreat Ave, Hartford, CT 06106, Office (860) 545-7298, Fax (860) 545-7797, emma.sprooten@yale.edu.

population, and verified its relevance to schizophrenia in an independent case-control sample. Secondly, we showed that the neuroanatomical variation defined by this component is largely determined by additive genetic variation ($h^2 = 0.59$), and genome-wide linkage analysis resulted in a significant linkage peak at 12q24 ($LOD = 3.76$). This region has been of significant interest to psychiatric genetics as it contains the Darier's disease locus and other proposed susceptibility genes (e.g. *DAO*, *NOS1*), and it has been linked to affective disorders and schizophrenia in multiple populations. Thus, in conjunction with previous clinical studies, our data imply that one or more psychiatric risk variants at 12q24 are co-inherited with reductions in mPFC and insula gray matter concentration.

Keywords

Extended pedigrees; magnetic resonance imaging; insula; medial prefrontal cortex; quantitative trait locus

1. Introduction

Schizophrenia is a heritable disorder (Sullivan et al., 2003) but the genetic variation accounting for its inheritance is complex and difficult to characterize. Many genetic markers, both common and rare, are thought to contribute to genetic risk for schizophrenia and related disorders (Gratten et al., 2014). Efforts to localize susceptibility variants and investigate their downstream effects on protein synthesis and interactions are hindered by the heterogeneity and complexity of the clinical phenotype, and by the small effect sizes of the common variants typically identified by large-scale association studies. Family-based designs offer increased power to identify genetic variants, especially rare variants with potentially larger effect sizes (Williams and Blangero 1999). In addition, intermediate phenotypes that are heritable and genetically associated with a clinical diagnosis can facilitate variant localization, both because of their quantitative nature and because of their assumed proximity to the genetic effects (Glahn et al., 2007; Gottesman and Gould 2003). Simultaneously, these endophenotypes (Gottesman and Gould 2003) provide insights into the variants' influences on biological processes, yielding clues to pathological mechanisms that contribute to the expression of the clinical phenotype.

Neuroanatomical traits derived from magnetic resonance imaging (MRI) are logical endophenotypes as their selection can be informed by a large body of literature in clinical samples, and they are likely to be biologically intermediate between genes' functions and their more remote effects on behavioral phenotypes (Glahn et al., 2007). Despite marked clinical and methodological heterogeneity, multiple meta-analyses of voxel-based morphometry studies in schizophrenia have identified the insula and the medial prefrontal cortex (mPFC) as the neuroanatomical regions most consistently associated with schizophrenia across all published case-control studies (Bora et al., 2011; Fornito et al., 2009; Glahn et al., 2008; Palaniyappan et al., 2012; Shepherd et al., 2012).

Source-based morphometry (SBM) (Xu et al., 2009) is a multivariate method that decomposes gray matter concentration images, derived from T_1-weighted MRI scans, into spatially independent sources. The outcome is a matrix of weights for each individual on

each source map, which can be used as dependent variables instead of voxel-wise values. As such, SBM dramatically reduces the number of comparisons typically performed in voxel-based analyses. SBM also addresses other common problems in MRI analysis, including the choice of smoothness kernel and the non-stationarity of image smoothness (Hayasaka and Nichols 2003). Remarkably, the application of SBM has repeatedly identified a single component comprising the mPFC and the insula – the same regions as the case-control meta-analyses (15-19) – as the most affected anatomical network in schizophrenia patients (Gupta et al., In Press; Kasparek et al., 2010; Turner et al., 2012; Xu et al., 2009). Thus, following an endophenotype strategy, quantification and localization of the genetic influences on this schizophrenia-associated neuroanatomical trait could provide testable candidate genes and generate novel hypotheses about mechanisms underlying susceptibility for schizophrenia.

Here, we used SBM in a large sample of randomly ascertained pedigrees. Our aims were threefold: (1) to replicate the schizophrenia-associated insula-mPFC source as a spatially independent component in a new sample representative of the general population; (2) to estimate its heritability; and (3) to localize this genetic influence to specific genomic regions using linkage analysis.

2. Materials and Methods

2.1 GOBS extended pedigree sample

Participants were individuals of Mexican American ancestry who took part in the Genetics Of Brain Structure and Function Study (GOBS) (McKay et al., 2014; Olvera et al., 2011), which is an extension of the San Antonio Family study (Mitchell et al., 1996). Individuals were randomly selected from the community with the only constraints that they were part of a large family of Mexican-American ancestry and lived within the San Antonio region. For the present analysis, subjects were excluded for MRI contraindications, documented medical history of neurological illness, or any neurological event visible on the T_1-weighted scans (see section 2.3). Of the participants in the final analysis, 22 self-reported history of a neurological event or illness (18 stroke, 1 Parkinson's disease, 3 multiple sclerosis, 1 brain surgery), but excluding these individuals did not change the pattern of results presented. After quality control procedures (see below) T_1-weighted scans were available for 887 individuals (532 female), from 69 pedigrees ranging from 2 to 90 family members, and 46 singletons. Participants were between 18 and 85 years old (mean= 44; standard deviation(SD)=15).

History of axis-1 disorders was assessed using the Mini International Neuropsychiatric Interview (Sheehan et al., 1998). Of the individuals included in the main analysis, four had a diagnosis of schizophrenia, fifteen of bipolar disorder, and four of schizoaffective disorder. For our main results, we performed additional analyses excluding these individuals (see results section). Additionally, 297 participants had a history of major depression, and 118 had a history of an anxiety disorder, and we performed additional analyses co-varying for these diagnoses.

2.2 MR imaging and processing in GOBS

An MRI protocol optimized for cortical gray matter measurements (Kochunov and Davis 2009), with a retrospective motion correction technique (Kochunov et al., 2006), was used. For each participant, seven T_1-weighted scans were obtained in a Siemens 3 Tesla Trio scanner located at the Research Imaging Institute, University of Texas Health Science Center, using a magnetization prepared sequence with an adiabatic inversion contrast-forming pulse (scan parameters: TE/TR/TI=3.04/2100/785 ms, flip angle=11 degrees). As in (Kochunov et al., 2006), for each subject the seven volumes were coregistered and averaged.

Upon visual inspection, five individuals were excluded for neurological abnormalities, and one for a scanner artifact. The resulting images were further processed in SPM5 (http://www.fil.ion.ucl.ac.uk/spm/software/spm5/), using the same parameters as in Turner et al. (Gupta et al., In Press; Turner et al., 2012) and Xu et al. (Xu et al., 2009). Gray matter maps were nonlinearly normalized, resliced to a 2mm^3 MNI template and segmented into gray matter, white matter and cerebrospinal fluid (Ashburner and Friston 2000). The accuracy of the segmentations and normalizations was ensured by visual inspection and by calculating correlations with the average normalized gray matter map for the entire sample. Five individuals were excluded because of segmentation or normalization problems.

2.3 Source-based morphometry

SBM (Kasparek et al. 2010, ; Xu et al., 2009) (http://mialab.mrn.org/software/gift/) is a multivariate method that decomposes structural images into spatially distinct sources using independent component analysis (Bell and Sejnowski 1995). The decomposition of the subject-by-voxel matrix (X) results in a subject-by-component mixing matrix (W), which contains the weights of the subjects on each component; and a component-by-voxel source matrix (C), which contains the loadings of each voxel for each component. This decomposition[1] can be noted as follows (Calhoun et al., 2001):

$$X = W^* C$$

And therefore:

$$W = X^* C^{-1}$$

For a subject i, the weight of a component j reflects the overall gray matter concentration for that component map of n voxels. More quantitatively, the weight can be conceived of as the sum of each voxel's observed gray matter value multiplied by each voxel's loading on the component:

$$W_{i,j} = \sum_{k=1}^{n} X_{i,k} C_{k,j}^{-1}$$

---

[1]In practice this decomposition of interest is preceded by an initial principal component analysis step on the subject-by-voxel matrix X to obtain a square matrix RX, as explained in Calhoun et al. (32). For clarity we have omitted this step from the current explanation and also note the inverse of C as C^{-1} even though it would technically be non-square if we omitted the PCA step.

These weights can be used as dependent variables in subsequent analyses.

The optimal number of components for our data was estimated according to an information criteria algorithm (Li et al., 2007). To determine the stability of the decomposition, ICASSO (Himberg et al., 2004) was used, with random value initiation and bootstrapping options, for 20 repetitions.[2] The stability indices for all components were higher than 0.97.

2.4 Relevance to schizophrenia: application to an independent case-control cohort

While we had strong *a priori* evidence for the involvement of insula and mPFC gray matter in schizophrenia (Bora et al., 2011; Fornito et al., 2009; Glahn et al., 2008; Palaniyappan et al., 2012; Shepherd et al., 2012; Turner et al., 2012), we also directly verified the relevance of the currently derived component to brain morphology of schizophrenia in a separate dataset of 936 healthy control participants (HC) and 784 patients with schizophrenia (SCZ), aggregated from 8 independent studies. More detailed information about the case-control sample are presented in the Supplementary Materials and in Gupta et al. (Gupta et al., In Press).

Using spatial-temporal regression, a method available in the SBM toolbox, we obtained weighting scores for each individual in the case-control dataset for the components identified using the GOBS data. By entering these as the dependent variable in a regression with study site, diagnosis and their interactions as factors, we tested directly whether gray matter concentration defined by the component extracted from the GOBS dataset was reduced in patients with schizophrenia.

In addition, we quantified the similarity between the components derived from the GOBS and the case-control datasets by calculating (1) pairwise correlations of the voxel loading values across maps from both datasets; and (2) Dice coefficients of the thresholded maps at z>3, where the Dice coefficient is defined as twice the number of voxels with the same value in both maps divided by total number of voxels (within the masks).

2.5 Heritability analysis

All quantitative genetics analyses were performed in SOLAR (Almasy and Blangero 1998), which decomposes the variance of a trait into genetic and environmental components by modeling the covariance between individuals as a function of their genetic proximity. Typically, the trait variance is decomposed into an additive genetic effects (heritability), covariate effects (sex, age, age^2, age $\times$ sex, age$^2 \times$ sex), and residual environmental effects. We also tested for cubic effects of age, but these were negligible (p > 0.9) and dropped from the model. The significance of each variance component is assessed by a likelihood-ratio test comparing the final model to the model without the variable of interest. Using the subject's weights on the insula-mPFC component as a trait, this method yielded an index of the overall heritability (h^2) of gray matter concentration within the anatomical regions of the component. Prior to running SOLAR, eight outliers (mean+− 3*SD) were removed from the

---

[2]Note that in this case bootstrapping is applied to estimate the degree of variability across iterations, and not – as commonly is the case - to estimate a null-distribution, which would require many more iterations.

data and the remaining weights were transformed using an inverse normalization transformation.

2.6 Linkage and association analyses

Linkage analysis was performed in SOLAR, by adding location-specific identity-by-descent (IBD) information to the above heritability model. IBD means that two individuals within the same pedigree not only share the same genotype, but also inherited it from the same founder. Here, for the GOBS pedigrees the IBD matrices were estimated as in Curren et al. (2013), using the Loki package (Heath et al., 1997). In brief, for 15,000 SNPs[3] across the genome, which were selected to be in linkage equilibrium (r<0.2), Loki applies Marcov Chain Monte Carlo sampling methods to empirically estimate the pairwise IBD probabilities for each SNP between each individual (Heath et al., 1997).

The significance of the contribution of each locus is quantified by a LOD score, defined as the logarithm (base 10) of the ratio of the likelihood of the model with the locus-specific IBD matrix to the model without this component (i.e. the same model used to test heritability). The LOD threshold for genome-wide significance was determined a priori for the complex pedigree structure of GOBS. This calculation is based on Gaussian models of the probability of crossover rates under the null distribution (Feingold et al., 1993), given our pedigree structure, the number of SNPs in our IBD matrix and known Haldane maps. Given our pedigree structure and distribution of markers, a LOD of 2.9 is required for genome-wide significant linkage (genome-wide $\alpha < 0.05$).

To further determine whether any specific SNPs were driving the observed linkage, association analysis was performed for all common SNPs under the linkage peak (defined as all consecutive loci with LODs greater than half the maximum LOD). DNA was extracted from lymphocytes, genotyped using Illumina beadchips (Human1M-Duo Beadchip; or HumanHap550 BeadChip in tandem with HumanHap450S Beadchip), and checked for accordance with Mendelian consistency as described previously (Sprooten et al., 2014). To account for pedigree structure, association analysis was performed in SOLAR, using methods identical to (Sprooten et al., 2014). In brief, the minor allele dosage of each tagging SNP is added as a covariate to the model used for heritability. A corrected p-value was calculated according to family-wise error rate at 5%, by calculating in SOLAR the effective number of independent SNPs under the peak, adjusted for linkage disequilibrium (LD) (Moskvina and Schmidt 2008).

3. Results

3.1 Identification and validation of insula-mPFC component

The method of Li (Li et al., 2007) estimated that the GOBS gray matter images were optimally explained by 21 independent sources.

---

[3]Note that here the SNPs are not used to test for association testing, but merely to represent an independent locus for IBD estimation to perform linkage.

As hypothesized, one component (Figure 1) closely resembled the insula-mPFC clusters resulting from the aforementioned voxel-based morphometry meta-analyses (Bora et al., 2011 ; Palaniyappan et al., 2012; Shepherd et al., 2012), as well as previous SBM studies (Gupta et al., In Press; Turner et al., 2012; Xu et al., 2009). The bilateral insular parts of this component contained voxels in the insula and temporal pole, extending to the inferior frontal, orbitofrontal, opercular and superior temporal gyri. The frontal cluster of the component contained voxels in the anterior cingulate and paracingulate gyrus, frontal pole, medial frontal cortex and superior frontal gyrus. A small number of voxels were negatively correlated with the mPFC and insula, mostly containing white matter in the superior parietal lobes and splenium.

In line with qualitative comparisons to the literature, spatio-temporal regression in the case-control dataset revealed that the weights on this insula-mPFC component were highly significantly different between schizophrenia patients and healthy participants ($F = 292.69$, $p = 1.19*10^{-60}$), in the absence of site-by-diagnosis interactions ($F=1.24$, $p=0.22$). The correlation coefficient of the loadings across voxels between this map and the map derived from the case-control data was 0.58 and the Dice coefficient was 0.97, both indicating a high degree of overlap.

The present paper focuses on the insula-mPFC cluster. We provide information about all 21 component maps including heritability estimates and case-control statistics in the Supplementary Materials.

3.2 Quantitative trait localization

The polygenic model in SOLAR using the weights of the insula-mPFC component as quantitative trait revealed that gray matter in this region is significantly heritable ($h^2=0.59$; p=$1.78*10^{-15}$). Linkage analysis resulted in a genome-wide significant peak on chromosome 12 at 12q24 (12q24.11-12q24.23; maximum LOD=3.76; Figure 2).

The linkage peak contained 392 tagging SNPs. Taking into account LD, the peak-wide corrected p-value for SNP associations was $1.64*10^{-4}$. None of the SNPs were peak-wide significant (Supplementary Figure 2). The strongest association (p=$7.71*10^{-4}$) was found for rs7133582, an intronic SNP in a transcription factor binding site in *KSR2*. Several other nearby SNPs had modest to strong associations with the insula-mPFC trait, altogether spanning 12q24.21 to 12q24.23.

Pedigree-specific LODs were all <1, indicating that linkage was not driven by any specific pedigree. The heritability and the linkage results remained similar when excluding individuals with self-reported history of neurological events or illness, schizophrenia, schizoaffective disorder and bipolar disorder ($h^2=0.52$; LOD=3.19); and when co-varying for history of anxiety disorders ($h^2 = 0.60$; LOD=3.06) and major depressive disorder ($h^2=0.60$; LOD=2.97). There were no significant effects of history of major depression (p > 0.8) or anxiety disorders ($p>0.3$) on the component's weights.

To further assess the value of the SBM approach, we also extracted gray matter concentration averages within a binarized mask of the component map (z > 3) for each

individual. This univariate phenotype was less heritable (h^2=0.47, p=3.08*10^{-11}), and the maximum LOD score on chromosome 12 was found at the same marker at 12q24 as the multivariate phenotype, but was much lower (LOD = 1.82).

4. Discussion

We used multivariate analyses of MRI images to extract a gray matter component comprising the insula and the mPFC, which have previously been shown be the most pronounced (Gupta et al., In Press; Turner et al., 2012) and most consistently implicated gray matter regions in schizophrenia (Bora et al., 2011; Fornito et al., 2009; Glahn et al., ; Palaniyappan et al., 2012; Shepherd et al., 2012). We directly confirmed that gray matter defined by our empirically derived component was reduced in patients with schizophrenia from an independent case-control sample. Next, we found that the overall gray matter concentration in this component is heritable, and following genome-wide linkage analysis, we identified a quantitative trait locus for this component at 12q24.

4.1 Replication and interpretation of insula-mPFC component

So far, SBM has been predominantly applied to case-control studies in schizophrenia (Gupta et al., In Press; Turner et al., ; Xu et al., 2009). Together these studies investigated three independent samples, in four separate analyses, all of which highlight the insula-mPFC component as the most important gray matter component in association with schizophrenia. The replication and heritability of this component in a sample representative of the general population supports the reliability of this technique, and indicates that gray-matter variation in this network is influenced by genetic factors.

The notion of the mPFC-insula as a coherent network is consistent with histological, anatomical, functional and developmental similarities between these regions. The insula and the mPFC display similarly high rates of cortical thickening during neonatal development (Lyall et al., 2014) and throughout childhood (Sowell et al., 2004). Histologically they are also similar, most notably because of the distinct and exclusive presence of von Economo neurons in these regions (Butti et al., 2013). As key regions of the limbic system, and more specifically the "salience network" (Seeley et al., 2007), the mPFC and insula interact intensely to serve higher-order cognitive processes such as social and self-awareness, intuition, error monitoring and interoception. As such, their dysfunction has been postulated to lie at the core of the experience of psychotic symptoms (Kapur 2003; Palaniyappan et al., 2012; Pu et al., 2012). In a complimentary theory, interactions between superior temporal, inferior frontal regions and the mPFC have long been hypothesized as key to the experience of auditory verbal hallucinations (Fletcher et al., 1999; Stephan et al., 2009).

4.2 Locus 12q24

We identified a 10Mb region at 12q24 linked to the insula-mPFC gray matter phenotype. This region has been of great interest to psychiatric genetics since Craddock et al. (Craddock et al., 1994) reported a cosegregation of bipolar disorder and Darier's disease, a skin disease that is caused by mutations in *ATP2A2* (Bashir et al., 1993; Craddock et al., 1993) (Supplementary Figure 2). Subsequently, dozens of studies reported linkage of 12q24 to

affective disorders in the UK, Ireland, Germany, Denmark, Canada, Iceland and Finland in locations spanning from 12q22 to 12q24 (Ekholm et al., 2003; Ewald et al., 2003; Jones et al., 2002; McInnis et al., ; Morissette et al., 1999). Fewer but better powered studies have linked schizophrenia to 12q24 with loci mostly concentrated in 12q24.11-12q24-31 (113-128 Mb; Assembly GRCh37/hg19) (Bulayeva et al., 2007; DeLisi et al., 2002; Faraone et al., 2006; Holmans et al., 2009; Moises et al., 1995; Williams et al., 2003). This narrowed region matches our mPFC-insula locus, as well as another linkage result in relation to neurocognitive performance in schizophrenia patients (Lien et al., 2010).

In our association study we were unable to localize our linkage signal to any specific variants. The strongest association was found for rs7133582, a SNP in a transcription factor binding site of *KSR2*, a functionally poorly characterized gene that is involved in the MAPK and ERK signaling pathways (Dougherty et al., 2009). Similarly, despite the considerable interest in the region, previous studies have not been able to unequivocally identify specific genes that may drive linkage results at 12q24. Although in the most recent genome-wide association analysis of schizophrenia the Psychiatric Genomics Consortium identified a top SNP in the Darier's gene *ATP2A2* with $p < 10^{-9}$ (Schizophrenia Working Group of the Psychiatric Genomics 2014), in the original Darier's disease pedigrees risk for psychiatric disorders did not map to *ATP2A2* itself (Jacobsen et al., 2001) and the co-segregation of psychiatric symptoms with Darier's disease was thought to be due to nearby variation in LD (Jones et al., 2002). Other efforts to identify specific neuropsychiatric risk genes at 12q24 overall yielded inconclusive results (Dawson et al., 1995; Green et al., 2005; Green et al., 2009; Jacobsen et al., 1996; Shink et al., 2005). Several large-scale family studies highlight the genetic heterogeneity at 12q24 (Bulayeva et al., 2007; McInnis et al., 2003; Shink et al., 2005), and it has been suggested that the wider 12q23-12q24 region contains multiple genes that may influence neuropsychiatric phenotypes (Barden et al., 2006; Shink et al., 2005). The original fine-mapping studies suggested *CUX2*, *FAM109A* (or FLJ32356) (Glaser et al., 2005), *P2RX7, CAMKK2,* (Barden et al., 2006), and *LINC00944* ("Slynar gene") (Buttenschon et al., 2010; Kalsi et al., 2006). However 12q24 also contains the schizophrenia candidate genes *DAO* (Verrall et al., 2010) and *NOS1* (Cui et al., ; Silberberg et al., 2010; Wockner et al., 2014). Interestingly, during fetal development *NOS1* is transiently highly expressed in the mPFC and insula only (Funk and Kwan 2014), and variants in *NOS1* have been associated with prefrontal morphology and function (Rose et al., 2012). Finally, rs7294919, the genome-wide association with hippocampal volume identified by the ENIGMA and CHARGE consortia (Bis et al., 2012; Stein et al., 2012) also lies under our peak.

4.3 Strengths and limitations

An advantage of our multivariate voxel-based analysis is that it gave rise to a reliably identifiable and data-driven single trait that was known to be relevant to schizophrenia based on a large body of pre-existing literature. However, a limitation of all voxel-based techniques is that the concentration values bear an indirect relationship to the physiological, morphological and cellular properties within each voxel. Both regional thickness and surface area contribute independently to voxel-wise gray matter concentrations (Rimol et al., 2012; Winkler et al., 2010), and likely local cortical curvature and white matter morphology also

play a role. As such, an understanding of the biological mechanisms of the genetic effects we identified requires further specification of the morphological properties that contribute to the schizophrenia-related phenotype we investigated here.

Secondly, there is a multitude of *a priori* evidence and a strong rationale for the relevance of our quantitative trait to schizophrenia, which we also directly confirmed in an independent case-control dataset. However, a limitation of our study, as of most intermediate phenotype studies, is that neither endophenotype-disease associations nor quantitative genetics analyses directly test the assumption that the endophenotype lies on the *causal* pathway from genetic risk variants to development of disease. This is a general limitation of the field that can only truly be addressed by longitudinal designs, which are difficult to obtain to the same quantity as the data we present here, and to this date lack the statistical power and/or suitable pedigree structures for gene localization and identification.

Thirdly, while our linkage peak was not driven by any specific families within our sample, the detection of a genetic signal that is potentially obscured by locus heterogeneity (whether caused by rare or common variants) is likely facilitated by the use of a quantitative intermediate phenotype and the recruitment of large pedigrees. However, as discussed, we were unable to localize the genetic effects to any specific genes or variants. Large-scale family-based analysis of deep sequence data may be necessary to obtain more definitive answers regarding which and to what extent specific genes at 12q24 influence brain morphology and neuropsychiatric phenotypes.

4.4 Conclusions

There is compelling evidence that gray matter concentration in the insula and mPFC is reduced in patients with schizophrenia and in their unaffected family members. The genomic region 12q24 has been linked to psychiatric disorders in multiple populations worldwide and contains many genes of interest for neuropsychiatric phenotypes. Our findings indicate that genetic variation in this region also contributes to gray matter concentration in the insula and mPFC in the general population. Thus, mPFC and insula morphology are likely neuroanatomical correlates of schizophrenia that are co-inherited with schizophrenia susceptibility variants at 12q24.

Supplementary Material

Refer to Web version on PubMed Central for supplementary material.

Acknowledgments

References

Almasy L, Blangero J. Multipoint quantitative-trait linkage analysis in general pedigrees. American journal of human genetics. 1998; 62(5):1198–1211. [PubMed: 9545414]

Ashburner J, Friston KJ. Voxel-based morphometry--the methods. NeuroImage. 2000; 11(6 Pt 1):805–821. [PubMed: 10860804]

Barden N, Harvey M, Gagne B, Shink E, Tremblay M, Raymond C, Labbe M, Villeneuve A, Rochette D, Bordeleau L, Stadler H, Holsboer F, Muller-Myhsok B. Analysis of single nucleotide polymorphisms in genes in the chromosome 12Q24.31 region points to P2RX7 as a susceptibility gene to bipolar affective disorder. American journal of medical genetics Part B, Neuropsychiatric genetics : the official publication of the International Society of Psychiatric Genetics. 2006; 141B(4):374–382.

Bashir R, Munro CS, Mason S, Stephenson A, Rees JL, Strachan T. Localisation of a gene for Darier's disease. Human molecular genetics. 1993; 2(11):1937–1939. [PubMed: 7506604]

Bell AJ, Sejnowski TJ. An information-maximization approach to blind separation and blind deconvolution. Neural computation. 1995; 7(6):1129–1159. [PubMed: 7584893]

Bis JC, DeCarli C, Smith AV, van der Lijn F, Crivello F, Fornage M, Debette S, Shulman JM, Schmidt H, Srikanth V, Schuur M, Yu L, Choi SH, Sigurdsson S, Verhaaren BF, DeStefano AL, Lambert JC, Jack CR Jr. Struchalin M, Stankovich J, Ibrahim-Verbaas CA, Fleischman D, Zijdenbos A, den Heijer T, Mazoyer B, Coker LH, Enzinger C, Danoy P, Amin N, Arfanakis K, van Buchem MA, de Bruijn RF, Beiser A, Dufouil C, Huang J, Cavalieri M, Thomson R, Niessen WJ, Chibnik LB, Gislason GK, Hofman A, Pikula A, Amouyel P, Freeman KB, Phan TG, Oostra BA, Stein JL, Medland SE, Vasquez AA, Hibar DP, Wright MJ, Franke B, Martin NG, Thompson PM, Enhancing Neuro Imaging Genetics through Meta-Analysis C; Nalls MA, Uitterlinden AG, Au R, Elbaz A, Beare RJ, van Swieten JC, Lopez OL, Harris TB, Chouraki V, Breteler MM, De Jager PL, Becker JT, Vernooij MW, Knopman D, Fazekas F, Wolf PA, van der Lugt A, Gudnason V, Longstreth WT Jr. Brown MA, Bennett DA, van Duijn CM, Mosley TH, Schmidt R, Tzourio C, Launer LJ, Ikram MA, Seshadri S, Cohorts for H; Aging Research in Genomic Epidemiology C. Common variants at 12q14 and 12q24 are associated with hippocampal volume. Nature genetics. 2012; 44(5):545–551. [PubMed: 22504421]

Bora E, Fornito A, Radua J, Walterfang M, Seal M, Wood SJ, Yucel M, Velakoulis D, Pantelis C. Neuroanatomical abnormalities in schizophrenia: a multimodal voxelwise meta-analysis and meta-regression analysis. Schizophrenia research. 2011; 127(1-3):46–57. [PubMed: 21300524]

Bulayeva KB, Glatt SJ, Bulayev OA, Pavlova TA, Tsuang MT. Genome-wide linkage scan of schizophrenia: a cross-isolate study. Genomics. 2007; 89(2):167–177. [PubMed: 17140763]

Buttenschon HN, Foldager L, Flint TJ, Olsen IM, Deleuran T, Nyegaard M, Hansen MM, Kallunki P, Christensen KV, Blackwood DH, Muir WJ, Straarup SE, Als TD, Nordentoft M, Borglum AD, Mors O. Support for a bipolar affective disorder susceptibility locus on chromosome 12q24.3. Psychiatric genetics. 2010; 20(3):93–101. [PubMed: 20410851]

Butti C, Santos M, Uppal N, Hof PR. Von Economo neurons: clinical and evolutionary perspectives. Cortex; a journal devoted to the study of the nervous system and behavior. 2013; 49(1):312–326.

Calhoun VD, Adali T, Pearlson GD, Pekar JJ. Spatial and temporal independent component analysis of functional MRI data containing a pair of task-related waveforms. Human brain mapping. 2001; 13(1):43–53. [PubMed: 11284046]

Craddock N, Dawson E, Burge S, Parfitt L, Mant B, Roberts Q, Daniels J, Gill M, McGuffin P, Powell J, et al. The gene for Darier's disease maps to chromosome 12q23-q24.1. Human molecular genetics. 1993; 2(11):1941–1943. [PubMed: 8129825]

Craddock N, Owen M, Burge S, Kurian B, Thomas P, McGuffin P. Familial cosegregation of major affective disorder and Darier's disease (keratosis follicularis). The British journal of psychiatry : the journal of mental science. 1994; 164(3):355–358. [PubMed: 8199789]

Cui H, Nishiguchi N, Yanagi M, Fukutake M, Mouri K, Kitamura N, Hashimoto T, Shirakawa O, Hishimoto A. A putative cis-acting polymorphism in the NOS1 gene is associated with

schizophrenia and NOS1 immunoreactivity in the postmortem brain. Schizophrenia research. 2010; 121(1-3):172–178. [PubMed: 20605417]

Curran JE, McKay DR, Winkler AM, Olvera RL, Carless MA, Dyer TD, Kent JW Jr. Kochunov P, Sprooten E, Knowles EE, Comuzzie AG, Fox PT, Almasy L, Duggirala R, Blangero J, Glahn DC. Identification of pleiotropic genetic effects on obesity and brain anatomy. Human heredity. 2013; 75(2-4):136–143. [PubMed: 24081229]

Dawson E, Gill M, Curtis D, Castle D, Hunt N, Murray R, Powell J. Genetic association between alleles of pancreatic phospholipase A2 gene and bipolar affective disorder. Psychiatric genetics. 1995; 5(4):177–180. [PubMed: 8750360]

DeLisi LE, Shaw SH, Crow TJ, Shields G, Smith AB, Larach VW, Wellman N, Loftus J, Nanthakumar B, Razi K, Stewart J, Comazzi M, Vita A, Heffner T, Sherrington R. A genome-wide scan for linkage to chromosomal regions in 382 sibling pairs with schizophrenia or schizoaffective disorder. The American journal of psychiatry. 2002; 159(5):803–812. [PubMed: 11986135]

Dougherty MK, Ritt DA, Zhou M, Specht SI, Monson DM, Veenstra TD, Morrison DK. KSR2 is a calcineurin substrate that promotes ERK cascade activation in response to calcium signals. Molecular cell. 2009; 34(6):652–662. [PubMed: 19560418]

Ekholm JM, Kieseppa T, Hiekkalinna T, Partonen T, Paunio T, Perola M, Ekelund J, Lonnqvist J, Pekkarinen-Ijas P, Peltonen L. Evidence of susceptibility loci on 4q32 and 16p12 for bipolar disorder. Human molecular genetics. 2003; 12(15):1907–1915. [PubMed: 12874110]

Ewald H, Kruse TA, Mors O. Genome wide scan using homozygosity mapping and linkage analyses of a single pedigree with affective disorder suggests oligogenic inheritance. American journal of medical genetics Part B, Neuropsychiatric genetics : the official publication of the International Society of Psychiatric Genetics. 2003; 120B(1):63–71.

Faraone SV, Hwu HG, Liu CM, Chen WJ, Tsuang MM, Liu SK, Shieh MH, Hwang TJ, Ou-Yang WC, Chen CY, Chen CC, Lin JJ, Chou FH, Chueh CM, Liu WM, Hall MH, Su J, Van Eerdewegh P, Tsuang MT. Genome scan of Han Chinese schizophrenia families from Taiwan: confirmation of linkage to 10q22.3. The American journal of psychiatry. 2006; 163(10):1760–1766. [PubMed: 17012687]

Feingold E, Brown PO, Siegmund D. Gaussian models for genetic linkage analysis using complete high-resolution maps of identity by descent. American journal of human genetics. 1993; 53(1):234–251. [PubMed: 8317489]

Fletcher P, McKenna PJ, Friston KJ, Frith CD, Dolan RJ. Abnormal cingulate modulation of fronto-temporal connectivity in schizophrenia. NeuroImage. 1999; 9(3):337–342. [PubMed: 10075903]

Fornito A, Yucel M, Patti J, Wood SJ, Pantelis C. Mapping grey matter reductions in schizophrenia: an anatomical likelihood estimation analysis of voxel-based morphometry studies. Schizophrenia research. 2009; 108(1-3):104–113. [PubMed: 19157788]

Funk OH, Kwan KY. Nitric oxide signaling in the development and evolution of language and cognitive circuits. Neuroscience research. 2014

Glahn DC, Laird AR, Ellison-Wright I, Thelen SM, Robinson JL, Lancaster JL, Bullmore E, Fox PT. Meta-analysis of gray matter anomalies in schizophrenia: application of anatomic likelihood estimation and network analysis. Biological psychiatry. 2008; 64(9):774–781. [PubMed: 18486104]

Glahn DC, Thompson PM, Blangero J. Neuroimaging endophenotypes: strategies for finding genes influencing brain structure and function. Human brain mapping. 2007; 28(6):488–501. [PubMed: 17440953]

Glaser B, Kirov G, Green E, Craddock N, Owen MJ. Linkage disequilibrium mapping of bipolar affective disorder at 12q23-q24 provides evidence for association at CUX2 and FLJ32356. American journal of medical genetics Part B, Neuropsychiatric genetics : the official publication of the International Society of Psychiatric Genetics. 2005; 132B(1):38–45.

Gottesman II, Gould TD. The endophenotype concept in psychiatry: etymology and strategic intentions. The American journal of psychiatry. 2003; 160(4):636–645. [PubMed: 12668349]

Gratten J, Wray NR, Keller MC, Visscher PM. Large-scale genomics unveils the genetic architecture of psychiatric disorders. Nature neuroscience. 2014; 17(6):782–790. [PubMed: 24866044]

Green E, Elvidge G, Jacobsen N, Glaser B, Jones I, O'Donovan MC, Kirov G, Owen MJ, Craddock N. Localization of bipolar susceptibility locus by molecular genetic analysis of the chromosome 12q23-q24 region in two pedigrees with bipolar disorder and Darier's disease. The American journal of psychiatry. 2005; 162(1):35–42. [PubMed: 15625199]

Green EK, Grozeva D, Raybould R, Elvidge G, Macgregor S, Craig I, Farmer A, McGuffin P, Forty L, Jones L, Jones I, O'Donovan MC, Owen MJ, Kirov G, Craddock N. P2RX7: A bipolar and unipolar disorder candidate susceptibility gene? American journal of medical genetics Part B, Neuropsychiatric genetics : the official publication of the International Society of Psychiatric Genetics. 2009; 150B(8):1063–1069.

Gupta CN, Calhoun VD, Rachkona S, Chen J, Liu J, Segall J, Franke B, Zwiers M, Aias-Vasquez A, Buitelaar J, Fischer S, Fernandez G, van Erp TGM, Potkin S, Ford J, Mathalon D, McEwen S, Lee JH, Mueller BA, Greve DN, Andreassen O, Agartz I, Gollub RL, Sponheim SR, Ehrlich S, Wang L, Pearlson G, Glahn DC, Sprooten E, Mayer AR, Stephen J, Jung RE, Canive J, Bustillo J, Turner JA. Patterns of gray matter abnormalities in schizophrenia based on an international mega-analysis. Schizophrenia bulletin. In Press.

Heath SC. Markov Chain Segregation and Linkage Analysis for Oligogenic Models. Am J Human Genet. 1997; 61:748–760. [PubMed: 9326339]

Hayasaka S, Nichols TE. Validating cluster size inference: random field and permutation methods. NeuroImage. 2003; 20(4):2343–2356. [PubMed: 14683734]

Himberg J, Hyvarinen A, Esposito F. Validating the independent components of neuroimaging time series via clustering and visualization. NeuroImage. 2004; 22(3):1214–1222. [PubMed: 15219593]

Holmans PA, Riley B, Pulver AE, Owen MJ, Wildenauer DB, Gejman PV, Mowry BJ, Laurent C, Kendler KS, Nestadt G, Williams NM, Schwab SG, Sanders AR, Nertney D, Mallet J, Wormley B, Lasseter VK, O'Donovan MC, Duan J, Albus M, Alexander M, Godard S, Ribble R, Liang KY, Norton N, Maier W, Papadimitriou G, Walsh D, Jay M, O'Neill A, Lerer FB, Dikeos D, Crowe RR, Silverman JM, Levinson DF. Genomewide linkage scan of schizophrenia in a large multicenter pedigree sample using single nucleotide polymorphisms. Molecular psychiatry. 2009; 14(8):786–795. [PubMed: 19223858]

Jacobsen N, Daniels J, Moorhead S, Harrison D, Feldman E, McGuffin P, Owen MJ, Craddock N. Association study of bipolar disorder at the phospholipase A2 gene (PLA2A) in the Darier's disease (DAR) region of chromosome 12q23-q24.1. Psychiatric genetics. 1996; 6(4):195–199. [PubMed: 9149325]

Jacobsen NJ, Franks EK, Elvidge G, Jones I, McCandless F, O'Donovan MC, Owen MJ, Craddock N. Exclusion of the Darier's disease gene, ATP2A2, as a common susceptibility gene for bipolar disorder. Molecular psychiatry. 2001; 6(1):92–97. [PubMed: 11244492]

Jones I, Jacobsen N, Green EK, Elvidge GP, Owen MJ, Craddock N. Evidence for familial cosegregation of major affective disorder and genetic markers flanking the gene for Darier's disease. Molecular psychiatry. 2002; 7(4):424–427. [PubMed: 11986988]

Kalsi G, McQuillin A, Degn B, Lundorf MD, Bass NJ, Lawrence J, Choudhury K, Puri V, Nyegaard M, Curtis D, Mors O, Kruse T, Kerwin S, Gurling H. Identification of the Slynar gene (AY070435) and related brain expressed sequences as a candidate gene for susceptibility to affective disorders through allelic and haplotypic association with bipolar disorder on chromosome 12q24. The American journal of psychiatry. 2006; 163(10):1767–1776. [PubMed: 17012688]

Kapur S. Psychosis as a state of aberrant salience: a framework linking biology, phenomenology, and pharmacology in schizophrenia. The American journal of psychiatry. 2003; 160(1):13–23. [PubMed: 12505794]

Kasparek T, Marecek R, Schwarz D, Prikryl R, Vanicek J, Mikl M, Ceskova E. Source-based morphometry of gray matter volume in men with first-episode schizophrenia. Human brain mapping. 2010; 31(2):300–310. [PubMed: 19777553]

Kochunov P, Davis M. Development of structural MR brain imaging protocols to study genetics and maturation. Methods. 2009; 50(3):136–146. [PubMed: 19665566]

Kochunov P, Lancaster JL, Glahn DC, Purdy D, Laird AR, Gao F, Fox P. Retrospective motion correction protocol for high-resolution anatomical MRI. Hum Brain Mapp. 2006; 27(12):957–962. [PubMed: 16628607]

Li YO, Adali T, Calhoun VD. Estimating the number of independent components for functional magnetic resonance imaging data. Human brain mapping. 2007; 28(11):1251–1266. [PubMed: 17274023]

Lien YJ, Liu CM, Faraone SV, Tsuang MT, Hwu HG, Hsiao PC, Chen WJ. A genome-wide quantitative trait loci scan of neurocognitive performances in families with schizophrenia. Genes, brain, and behavior. 2010; 9(7):695–702.

Lyall AE, Shi F, Geng X, Woolson S, Li G, Wang L, Hamer RM, Shen D, Gilmore JH. Dynamic Development of Regional Cortical Thickness and Surface Area in Early Childhood. Cerebral cortex. 2014

McInnis MG, Lan TH, Willour VL, McMahon FJ, Simpson SG, Addington AM, MacKinnon DF, Potash JB, Mahoney AT, Chellis J, Huo Y, Swift-Scanlan T, Chen H, Koskela R, Stine OC, Jamison KR, Holmans P, Folstein SE, Ranade K, Friddle C, Botstein D, Marr T, Beaty TH, Zandi P, DePaulo JR. Genome-wide scan of bipolar disorder in 65 pedigrees: supportive evidence for linkage at 8q24, 18q22, 4q32, 2p12, and 13q12. Molecular psychiatry. 2003; 8(3):288–298. [PubMed: 12660801]

McKay DR, Knowles EE, Winkler AA, Sprooten E, Kochunov P, Olvera RL, Curran JE, Kent JW Jr. Carless MA, Goring HH, Dyer TD, Duggirala R, Almasy L, Fox PT, Blangero J, Glahn DC. Influence of age, sex and genetic factors on the human brain. Brain imaging and behavior. 2014; 8(2):143–152. [PubMed: 24297733]

Mitchell BD, Kammerer CM, Blangero J, Mahaney MC, Rainwater DL, Dyke B, Hixson JE, Henkel RD, Sharp RM, Comuzzie AG, VandeBerg JL, Stern MP, MacCluer JW. Genetic and environmental contributions to cardiovascular risk factors in Mexican Americans. The San Antonio Family Heart Study. Circulation. 1996; 94(9):2159–2170. [PubMed: 8901667]

Moises HW, Yang L, Kristbjarnarson H, Wiese C, Byerley W, Macciardi F, Arolt V, Blackwood D, Liu X, Sjogren B, et al. An international two-stage genome-wide search for schizophrenia susceptibility genes. Nature genetics. 1995; 11(3):321–324. [PubMed: 7581457]

Morissette J, Villeneuve A, Bordeleau L, Rochette D, Laberge C, Gagne B, Laprise C, Bouchard G, Plante M, Gobeil L, Shink E, Weissenbach J, Barden N. Genome-wide search for linkage of bipolar affective disorders in a very large pedigree derived from a homogeneous population in quebec points to a locus of major effect on chromosome 12q23-q24. American journal of medical genetics. 1999; 88(5):567–587. [PubMed: 10490718]

Moskvina V, Schmidt KM. On multiple-testing correction in genome-wide association studies. Genetic epidemiology. 2008; 32(6):567–573. [PubMed: 18425821]

Olvera RL, Bearden CE, Velligan DI, Almasy L, Carless MA, Curran JE, Williamson DE, Duggirala R, Blangero J, Glahn DC. Common genetic influences on depression, alcohol, and substance use disorders in Mexican-American families. American journal of medical genetics Part B, Neuropsychiatric genetics : the official publication of the International Society of Psychiatric Genetics. 2011; 156B(5):561–568.

Palaniyappan L, Balain V, Liddle PF. The neuroanatomy of psychotic diathesis: a meta-analytic review. Journal of psychiatric research. 2012; 46(10):1249–1256. [PubMed: 22790253]

Pu W, Li L, Zhang H, Ouyang X, Liu H, Zhao J, Li L, Xue Z, Xu K, Tang H, Shan B, Liu Z, Wang F. Morphological and functional abnormalities of salience network in the early-stage of paranoid schizophrenia. Schizophrenia research. 2012; 141(1):15–21. [PubMed: 22910405]

Rimol LM, Nesvag R, Hagler DJ Jr. Bergmann O, Fennema-Notestine C, Hartberg CB, Haukvik UK, Lange E, Pung CJ, Server A, Melle I, Andreassen OA, Agartz I, Dale AM. Cortical volume, surface area, and thickness in schizophrenia and bipolar disorder. Biological psychiatry. 2012; 71(6):552–560. [PubMed: 22281121]

Rose EJ, Greene C, Kelly S, Morris DW, Robertson IH, Fahey C, Jacobson S, O'Doherty J, Newell FN, McGrath J, Bokde A, Garavan H, Frodl T, Gill M, Corvin AP, Donohoe G. The NOS1 variant rs6490121 is associated with variation in prefrontal function and grey matter density in healthy individuals. NeuroImage. 2012; 60(1):614–622. [PubMed: 22227051]

Schizophrenia Working Group of the Psychiatric Genomics C. Biological insights from 108 schizophrenia-associated genetic loci. Nature. 2014; 511(7510):421–427. [PubMed: 25056061]

Seeley WW, Menon V, Schatzberg AF, Keller J, Glover GH, Kenna H, Reiss AL, Greicius MD. Dissociable intrinsic connectivity networks for salience processing and executive control. The

Journal of neuroscience : the official journal of the Society for Neuroscience. 2007; 27(9):2349–2356. [PubMed: 17329432]

Sheehan DV, Lecrubier Y, Sheehan KH, Amorim P, Janavs J, Weiller E, Hergueta T, Baker R, Dunbar GC. The Mini-International Neuropsychiatric Interview (M.I.N.I.): the development and validation of a structured diagnostic psychiatric interview for DSM-IV and ICD-10. The Journal of clinical psychiatry. 1998; 59(Suppl 20):22–33. quiz 34-57. [PubMed: 9881538]

Shepherd AM, Laurens KR, Matheson SL, Carr VJ, Green MJ. Systematic meta-review and quality assessment of the structural brain alterations in schizophrenia. Neuroscience and biobehavioral reviews. 2012; 36(4):1342–1356. [PubMed: 22244985]

Shink E, Harvey M, Tremblay M, Gagne B, Belleau P, Raymond C, Labbe M, Dube MP, Lafreniere RG, Barden N. Analysis of microsatellite markers and single nucleotide polymorphisms in candidate genes for susceptibility to bipolar affective disorder in the chromosome 12Q24.31 region. American journal of medical genetics Part B, Neuropsychiatric genetics : the official publication of the International Society of Psychiatric Genetics. 2005; 135B(1):50–58.

Silberberg G, Ben-Shachar D, Navon R. Genetic analysis of nitric oxide synthase 1 variants in schizophrenia and bipolar disorder. American journal of medical genetics Part B, Neuropsychiatric genetics : the official publication of the International Society of Psychiatric Genetics. 2010; 153B(7):1318–1328.

Sowell ER, Thompson PM, Leonard CM, Welcome SE, Kan E, Toga AW. Longitudinal mapping of cortical thickness and brain growth in normal children. The Journal of neuroscience : the official journal of the Society for Neuroscience. 2004; 24(38):8223–8231. [PubMed: 15385605]

Sprooten E, Knowles EE, McKay DR, Goring HH, Curran JE, Kent JW Jr. Carless MA, Dyer TD, Drigalenko EI, Olvera RL, Fox PT, Almasy L, Duggirala R, Kochunov P, Blangero J, Glahn DC. Common genetic variants and gene expression associated with white matter microstructure in the human brain. NeuroImage. 2014; 97:252–261. [PubMed: 24736177]

Stein JL, Medland SE, Vasquez AA, Hibar DP, Senstad RE, Winkler AM, Toro R, Appel K, Bartecek R, Bergmann O, Bernard M, Brown AA, Cannon DM, Chakravarty MM, Christoforou A, Domin M, Grimm O, Hollinshead M, Holmes AJ, Homuth G, Hottenga JJ, Langan C, Lopez LM, Hansell NK, Hwang KS, Kim S, Laje G, Lee PH, Liu X, Loth E, Lourdusamy A, Mattingsdal M, Mohnke S, Maniega SM, Nho K, Nugent AC, O'Brien C, Papmeyer M, Putz B, Ramasamy A, Rasmussen J, Rijpkema M, Risacher SL, Roddey JC, Rose EJ, Ryten M, Shen L, Sprooten E, Strengman E, Teumer A, Trabzuni D, Turner J, van Eijk K, van Erp TG, van Tol MJ, Wittfeld K, Wolf C, Woudstra S, Aleman A, Alhusaini S, Almasy L, Binder EB, Brohawn DG, Cantor RM, Carless MA, Corvin A, Czisch M, Curran JE, Davies G, de Almeida MA, Delanty N, Depondt C, Duggirala R, Dyer TD, Erk S, Fagerness J, Fox PT, Freimer NB, Gill M, Goring HH, Hagler DJ, Hoehn D, Holsboer F, Hoogman M, Hosten N, Jahanshad N, Johnson MP, Kasperaviciute D, Kent JW Jr. Kochunov P, Lancaster JL, Lawrie SM, Liewald DC, Mandl R, Matarin M, Mattheisen M, Meisenzahl E, Melle I, Moses EK, Muhleisen TW, Nauck M, Nothen MM, Olvera RL, Pandolfo M, Pike GB, Puls R, Reinvang I, Renteria ME, Rietschel M, Roffman JL, Royle NA, Rujescu D, Savitz J, Schnack HG, Schnell K, Seiferth N, Smith C, Steen VM, Valdes Hernandez MC, Van den Heuvel M, van der Wee NJ, Van Haren NE, Veltman JA, Volzke H, Walker R, Westlye LT, Whelan CD, Agartz I, Boomsma DI, Cavalleri GL, Dale AM, Djurovic S, Drevets WC, Hagoort P, Hall J, Heinz A, Jack CR Jr. Foroud TM, Le Hellard S, Macciardi F, Montgomery GW, Poline JB, Porteous DJ, Sisodiya SM, Starr JM, Sussmann J, Toga AW, Veltman DJ, Walter H, Weiner MW, Alzheimer's Disease Neuroimaging I; Consortium E; Consortium I; Saguenay Youth Study G; Bis JC, Ikram MA, Smith AV, Gudnason V, Tzourio C, Vernooij MW, Launer LJ, DeCarli C, Seshadri S, Cohorts for H; Aging Research in Genomic Epidemiology C; Andreassen OA, Apostolova LG, Bastin ME, Blangero J, Brunner HG, Buckner RL, Cichon S, Coppola G, de Zubicaray GI, Deary IJ, Donohoe G, de Geus EJ, Espeseth T, Fernandez G, Glahn DC, Grabe HJ, Hardy J, Hulshoff Pol HE, Jenkinson M, Kahn RS, McDonald C, McIntosh AM, McMahon FJ, McMahon KL, Meyer-Lindenberg A, Morris DW, Muller-Myhsok B, Nichols TE, Ophoff RA, Paus T, Pausova Z, Penninx BW, Potkin SG, Samann PG, Saykin AJ, Schumann G, Smoller JW, Wardlaw JM, Weale ME, Martin NG, Franke B, Wright MJ, Thompson PM, Enhancing Neuro Imaging Genetics through Meta-Analysis C. Identification of common variants associated with human hippocampal and intracranial volumes. Nature genetics. 2012; 44(5):552–561. [PubMed: 22504417]

Stephan KE, Friston KJ, Frith CD. Dysconnection in schizophrenia: from abnormal synaptic plasticity to failures of self-monitoring. Schizophrenia bulletin. 2009; 35(3):509–527. [PubMed: 19155345]

Sullivan PF, Kendler KS, Neale MC. Schizophrenia as a complex trait: evidence from a meta-analysis of twin studies. Archives of general psychiatry. 2003; 60(12):1187–1192. [PubMed: 14662550]

Turner JA, Calhoun VD, Michael A, van Erp TG, Ehrlich S, Segall JM, Gollub RL, Csernansky J, Potkin SG, Ho BC, Bustillo J, Schulz SC, Fbirn, Wang L. Heritability of multivariate gray matter measures in schizophrenia. Twin research and human genetics : the official journal of the International Society for Twin Studies. 2012; 15(3):324–335. [PubMed: 22856368]

Verrall L, Burnet PW, Betts JF, Harrison PJ. The neurobiology of D-amino acid oxidase and its involvement in schizophrenia. Molecular psychiatry. 2010; 15(2):122–137. [PubMed: 19786963]

Williams JT, Blangero J. Comparison of variance components and sibpair-based approaches to quantitative trait linkage analysis in unselected samples. Genetic epidemiology. 1999; 16(2):113–134. [PubMed: 10030396]

Williams NM, Norton N, Williams H, Ekholm B, Hamshere ML, Lindblom Y, Chowdari KV, Cardno AG, Zammit S, Jones LA, Murphy KC, Sanders RD, McCarthy G, Gray MY, Jones G, Holmans P, Nimgaonkar V, Adolfson R, Osby U, Terenius L, Sedvall G, O'Donovan MC, Owen MJ. A systematic genomewide linkage study in 353 sib pairs with schizophrenia. American journal of human genetics. 2003; 73(6):1355–1367. [PubMed: 14628288]

Winkler AM, Kochunov P, Blangero J, Almasy L, Zilles K, Fox PT, Duggirala R, Glahn DC. Cortical thickness or grey matter volume? The importance of selecting the phenotype for imaging genetics studies. NeuroImage. 2010; 53(3):1135–1146. [PubMed: 20006715]

Wockner LF, Noble EP, Lawford BR, Young RM, Morris CP, Whitehall VL, Voisey J. Genome-wide DNA methylation analysis of human brain tissue from schizophrenia patients. Translational psychiatry. 2014; 4:e339. [PubMed: 24399042]

Xu L, Groth KM, Pearlson G, Schretlen DJ, Calhoun VD. Source-based morphometry: the use of independent component analysis to identify gray matter differences with application to schizophrenia. Human brain mapping. 2009; 30(3):711–724. [PubMed: 18266214]
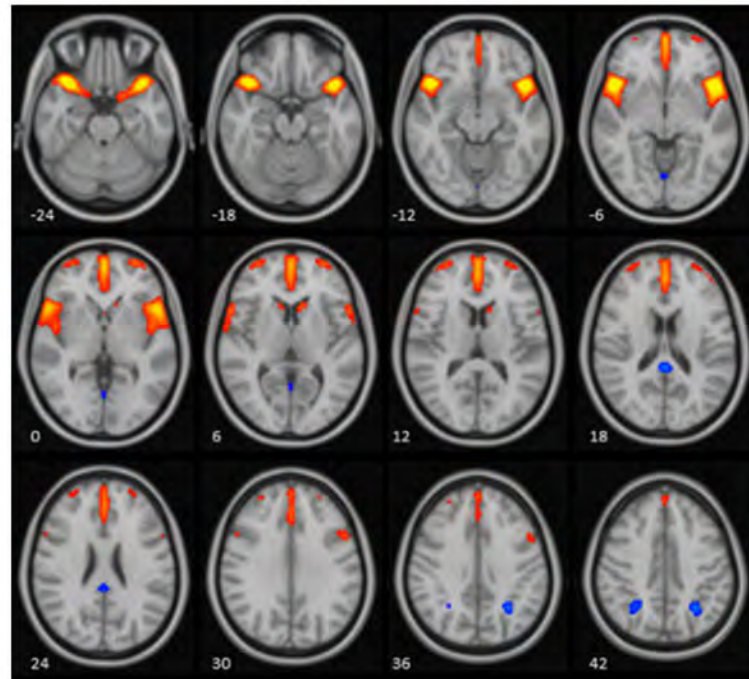
Figure 1. The insula-mPFC component derived from SBM analysis in GOBS
Insula-mPFC component map showing the voxels that primarily contribute to the component of interest, and that covary highly with one another across individuals in the GOBS sample. Voxels loading positively (z > 2.5) on the component are colored red-to-yellow, and voxels loading negatively (z < −2.5) are colored blue-to-light blue. Images are in radiological convention.
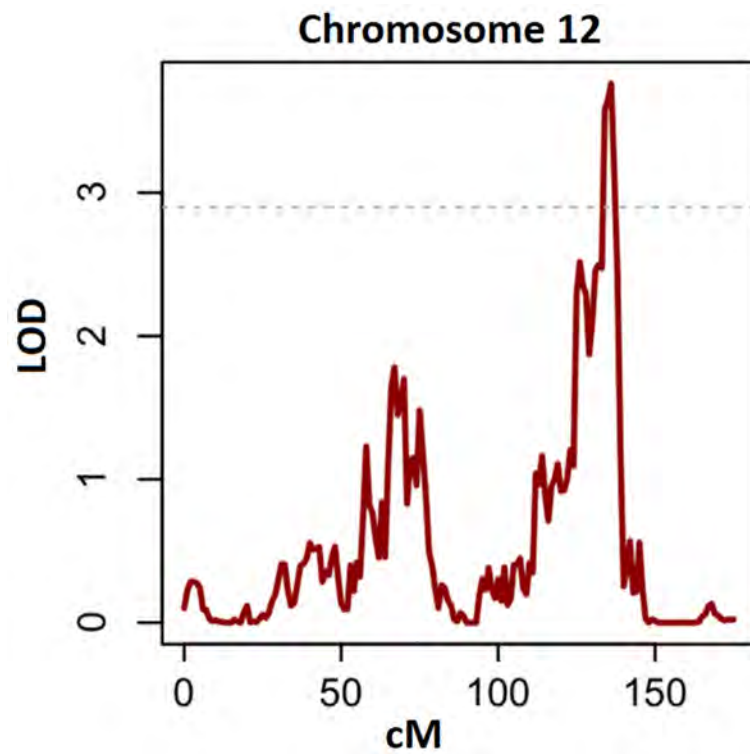
Figure 2. Linkage peak on chromosome 12 at 12q24 for weights on the insula - medial prefrontal cortex component

LOD scores plotted against location on chromosome 12. The maximum LOD is 3.76 at 12q24. The threshold for genome-wide significance is at 2.9, as indicated by the dashed line.

Neurobiology of Disease

Epigenetic Age Acceleration Assessed with Human White-Matter Images

Karen Hodgson,[1] Melanie A. Carless,[2] Hemant Kulkarni,[3] Joanne E. Curran,[3] Emma Sprooten,[4] Emma E. Knowles,[1] Samuel Mathias,[1] Harald H.H. Göring,[3] Nailin Yao,[1] Rene L. Olvera,[5] Peter T. Fox,[6] Laura Almasy,[3] Ravi Duggirala,[3] John Blangero,[3] and David C. Glahn[1,7]

[1]Department of Psychiatry, Yale University School of Medicine, New Haven, Connecticut 06511, [2]Department of Genetics, Texas Biomedical Research Institute, San Antonio, Texas 78227, [3]South Texas Diabetes and Obesity Institute, University of Texas Rio Grande Valley School of Medicine, Brownsville, Texas 78530, [4]Department of Psychiatry, Icahn Medical Institute, New York, New York 10029, [5]Department of Psychiatry, University of Texas Health Science Center San Antonio, San Antonio, Texas 78229, [6]Research Imaging Institute, University of Texas Health Science Center San Antonio, San Antonio, Texas 78229, and [7]Olin Neuropsychiatry Research Center, Institute of Living, Hartford Hospital, Hartford, Connecticut 06106

The accurate estimation of age using methylation data has proved a useful and heritable biomarker, with acceleration in epigenetic age predicting a number of age-related phenotypes. Measures of white matter integrity in the brain are also heritable and highly sensitive to both normal and pathological aging processes across adulthood. We consider the phenotypic and genetic interrelationships between epigenetic age acceleration and white matter integrity in humans. Our goal was to investigate processes that underlie interindividual variability in age-related changes in the brain. Using blood taken from a Mexican-American extended pedigree sample ($n = 628$; age = 23.28 –93.11 years), epigenetic age was estimated using the method developed by Horvath (2013). For $n = 376$ individuals, diffusion tensor imaging scans were also available. The interrelationship between epigenetic age acceleration and global white matter integrity was investigated with variance decomposition methods. To test for neuroanatomical specificity, 16 specific tracts were additionally considered. We observed negative phenotypic correlations between epigenetic age acceleration and global white matter tract integrity ($\rho_{\text{pheno}} = -0.119$, $p = 0.028$), with evidence of shared genetic ($\rho_{\text{gene}} = -0.463$, $p = 0.013$) but not environmental influences. Negative phenotypic and genetic correlations with age acceleration were also seen for a number of specific white matter tracts, along with additional negative phenotypic correlations between granulocyte abundance and white matter integrity. These findings (i.e., increased acceleration in epigenetic age in peripheral blood correlates with reduced white matter integrity in the brain and shares common genetic influences) provide a window into the neurobiology of aging processes within the brain and a potential biomarker of normal and pathological brain aging.

Key words: aging; epigenetics; genetics; white matter integrity

---

Significance Statement

Epigenetic measures can be used to predict age with a high degree of accuracy and so capture acceleration in biological age, relative to chronological age. The white matter tracts within the brain are also highly sensitive to aging processes. We show that increased biological aging (measured using epigenetic data from blood samples) is correlated with reduced integrity of white matter tracts within the human brain (measured using diffusion tensor imaging) with data from a large sample of Mexican-American families. Given the family design of the sample, we are also able to demonstrate that epigenetic aging and white matter tract integrity also share common genetic influences. Therefore, epigenetic age may be a potential, and accessible, biomarker of brain aging.

Introduction

The human population is aging at a rapid rate as the number of older persons have increased sharply within recent years (United Nations Department of Economic and Social Affairs Population Division, 2015). Between 2014 and 2060, the U.S. population of individuals over 65 year is expected to more than double, from

46.2 million to 98 million (Mather et al., 2015). An aging population brings with it an increasing urgency to understand the processes that lead to normal age-related decline in both physical and mental abilities as well as in age-associated illness. Given individual differences in the rate of age-related changes, the identification of biomarkers for vulnerability to deleterious aging effects and improved understanding of the mechanisms involved in healthy aging is invaluable. Among the more successful age-related biomarkers to date are indices based upon epigenetic variation (Fraga et al., 2005; Horvath et al., 2012; Hannum et al., 2013; Horvath, 2013; Teschendorff et al., 2013; Weidner et al., 2014; Jones et al., 2015), particularly the pan-tissue "epigenetic clock" developed by Horvath (2013). This clock is highly accurate in predicting age across a large number of different tissues, can be applied to data obtained for both the 27K and 450K Illumina Methylation BeadChips and has been shown to be predictive of a number of age-associated phenotypes (Horvath and Ritz, 2015; Marioni et al., 2015a, b).

The brain is of particular interest in aging, as cognitive decline is one of the greatest health threats of old age (van Boxtel et al., 1998). Additionally, the brain indirectly regulates aging responses in various organs (Bishop et al., 2010). Among *in vivo* measures of brain aging, white matter tract integrity (as indexed by fractional anisotropy [FA] from diffusion weighted MR images) is highly sensitive to both healthy and pathological aging (Moseley, 2002; Sullivan and Pfefferbaum, 2006; Giorgio et al., 2010; Teipel et al., 2010; Cox et al., 2016). Although FA measures are heritable (Jahanshad et al., 2013; Sprooten et al., 2014; Kochunov et al., 2015) and known to decline with age, Glahn et al. (2013) showed that genetic influences on white matter do not vary as a factor of age (no evidence for a gene by age interaction was found), in contrast with analyses for cognitive traits. Additionally, the specific biological mechanisms that influence white matter integrity are not yet known.

To determine whether variation in white matter integrity is associated with acceleration in epigenetic age, we analyzed their interrelationship in large, randomly ascertained pedigrees. Specifically, we calculated an estimator of epigenetic age for each subject, using a weighted average across 353 CpG sites (after Horvath) captured from blood samples. We then determined whether variation in this epigenetic age was correlated with variation in tract-based FA measures while controlling familial relationships (and after accounting for covariates of age, sex, and blood cell composition effects on epigenetic profiles). By using a family-based cohort, we considered not only phenotypic relationships, but also any underlying genetic correlations between these two heritable traits. We observed that accelerated epigenetic age was associated with reduced white matter integrity both globally and in a number of specific brain regions. This relationship was underpinned by shared genetic influences. We additionally investigated the relationship between epigenetic age acceleration and white matter hyperintensities, to consider the specificity of the relationship with FA.

Materials and Methods

Subjects. The Genetics of Brain Structure and Function study includes individuals recruited from large multigeneration Mexican-American families within San Antonio, Texas (Olvera et al., 2011). This is a subset of the San Antonio Family Study cohort, which was recruited pseudorandomly with the constraints that participants must live within the San Antonio region, be Mexican-American in ancestry, and have at least six first-degree relatives (Mitchell et al., 1996; Puppala et al., 2006). In this study, we considered the 628 individuals with epigenetic age estimates,

from 38 families (containing between 2–72 subjects, mean pedigree size = 14.25) and an additional 14 genetically unrelated spouses. Of these 628 subjects with epigenetic age estimates, 376 had diffusion tensor imaging (DTI) data also available. DTI scans were obtained on average 3.77 years (SD 1.61 years) after blood samples were drawn for the assessment of epigenetic methylation profiles. In all cases, the chronological age used is age at blood draw, but results are not substantially altered if this is substituted for age at DTI scan. Numbers reflect final totals after any individuals were removed during QC steps.

Epigenetic measures. Full details of methylation assays and preprocessing were described previously (Kulkarni et al., 2015). Briefly, peripheral blood samples were used to obtain 500 ng of DNA. Bisulfite conversion was performed; then methylation profiling was undertaken using the Infinium HumanMethylation450 BeadChip assay (Illumina). At each CpG site, methylation was quantified on a scale from 0 (fully unmethylated) to 1 (fully methylated). Probes that were located on the sex chromosomes ($n = 11,648$), in non-CpG loci ($n = 2994$), or contained SNPs ($n = 65$) were excluded.

Calculating epigenetic age and age acceleration. The method developed by Horvath (2013) was used to calculate epigenetic age for each individual using the available online age calculator (https://dnamage.genetics.ucla.edu). This approach uses DNA methylation levels of 353 age-predictive CpG sites (originally identified by Horvath, 2013, using an elastic net penalized regression model). This method has been shown to generate a predicted epigenetic age (labeled "DNAmAge" within the software) that correlates highly with chronological age and is accurate across a wide range of different cell and tissue types (Horvath, 2013), as well as being predictive of a number of age-associated phenotypes (Horvath and Ritz, 2015; Marioni et al., 2015a, b). Thus, epigenetic age, as captured with this method, is proposed to indicate the methylation-based age of a tissue.

In each model, the covariates of age, sex, age × sex, age², age² × sex, and the cell count estimates described below were applied to the epigenetic age ("DNAmAge") variable. Throughout the manuscript, we describe the variation in the epigenetic age that remains after accounting for these covariates as epigenetic age acceleration. Increased epigenetic age acceleration indicates that the individual is epigenetically older than would be expected given their chronological age and other covariates.

The epigenetic age calculator also calculated the predicted sex of each sample; 5 samples were excluded because of inconsistencies in reported and epigenetically predicted sex.

Estimating cell composition of whole blood samples. To consider the cell composition of the whole blood samples, previously developed methods for estimated cell counts (Houseman et al., 2012; Horvath, 2013) were used within the epigenetic calculator software, as recommended by Horvath (2013). Estimates of $CD8^+CD28^-CD45RA^-$ T cells, naive CD8 T cells, CD4 T cells, plasmablasts, natural killer cells, monocytes, and granulocytes were obtained and included as covariates when calculating epigenetic age acceleration.

Neuroimaging measures. White matter integrity was assessed using DTI. Scanning was performed using a multichannel head coil and Trio 3T system (Siemens) at the Research Imaging Institute, University of Texas Health Science Center (San Antonio, TX). The DTI acquisition protocol used a single-shot spin-echo, EPI sequence with a spatial resolution of 1.7×1.7 mm (repetition time/echo time = 8000/87 ms, FOV 200 mm, 55 nonparallel gradient directions b = 700 s/mm² and three non–diffusion-weighted images b = 0).

DTI scans were preprocessed using standard FSL pipelines (http://fsl.fmrib.ox.ac.uk/fsl/fslwiki/FDT). The resulting FA images were processed with tract-based spatial statistics (Smith et al., 2006). Images were nonlinearly registered to standard space, then averaged, and skeletonized to create a study-specific tract-based spatial statistics template (binarized at FA > 0.2). Next, the maximum nearby FA voxel was projected onto the skeleton, resulting in one skeleton image per subject, reflecting FA values of the centers of the white matter structure for that individual. The mean FA from the whole white matter skeleton was extracted for each individual to give a global measure of white matter integrity. In addition, for each subject, mean FA values were extracted from each region and averaged across hemispheres for 16 specific tracts as defined by the Johns Hopkins White Matter Atlas (Mori et al., 2008).

Fluid Attenuated Inversion Recovery images were obtained using the following parameters: TR/TE/TI/flip angle/ETL = 5 s/353 ms/1.8 s/180°/221. Preprocessing involved the removable of nonbrain tissue, registration to the Talairach frame, and RF inhomogeneity correction. Then, an experienced neuroanatomist used in-house software (http://ric.uthscsa.edu/mango) to manually delineate white matter hyperintensities. This was completed with high ($r > 0.9$) test-retest reliability. These methods have been previously described in detail (Kochunov et al., 2010). Whole brain white matter hyperintensity volumes were used.

Statistical analysis. Using SOLAR (Sequential Oligogenic Linkage Analysis Routines), first the heritability of epigenetic age acceleration and each DTI trait was calculated. As the global measure of white matter integrity includes FA estimates across the brain, including more peripheral FA not captured by the 16 specific Johns Hopkins White Matter Atlas tracts, our primary outcome was the phenotypic correlation between epigenetic age acceleration and global white matter tract integrity, as determined within a bivariate model. This phenotypic relationship was decomposed to give genetic and environmental correlations. To assess neuroanatomical specificity, we then examined the relationship between epigenetic age acceleration and each of the 16 specific DTI tracts. Phenotypic correlations where $p < 0.05$ were considered suggestive, and we applied a false discovery rate (FDR) correction (Benjamini and Hochberg, 1995) across the 16 specific tracts to account for multiple hypothesis testing (phenotypic correlations where FDR < 0.05 was considered significant). All phenotypic correlations reaching at least suggestive significance were decomposed into genetic and environmental components.

Covariates in each model were age, sex, age × sex, age^2, and age^2 × sex. Additionally, for epigenetic age acceleration, covariates of cell marker abundance were also applied (given the effect of cell heterogeneity on methylation data from whole blood).

Results

Epigenetic age

The estimated epigenetic age ("DNAmAge") of the sample ranged between 20.42 and 86.48 years (mean ± SD, 48.12 ± 11.49 years). At the time of blood draw, the chronological age of the sample ranged between 23.28 and 93.11 years (45.45 ± 13.30 years). These two variables show a high correlation ($\rho_{\text{pheno}} = 0.932$, $p = 1.82 \times 10^{-285}$), as depicted in Figure 1A. The average difference between epigenetic and chronological age is 2.67 years (so epigenetic age is typically higher than chronological age in this sample) When we consider females and males separately, the average difference between epigenetic and chronological age is 2.47 years in females and 3.04 years in males; but this difference does not reach significance in our sample (previous findings suggest the epigenetic aging rate of men is significantly higher than for women) (Horvath et al., 2016a). For the whole sample, the median absolute difference between epigenetic and chronological age is 3.68 years, indicating that epigenetic and chronological age differs by <3.68 years for 50% of the subjects. However, for some individuals, differences between epigenetic and chronological age were substantial; 7.00% of the sample have an absolute difference of >10 years, and the maximum absolute difference between epigenetic and chronological age is 15.96 years.

Epigenetic age acceleration index

As detailed in Materials and Methods, the epigenetic age acceleration measure captures variation in epigenetic age ("DNAmAge") estimates, after accounting for covariates of chronological age, sex, age × sex, age^2, and age^2 × sex, and cell composition in the blood. Positive values for epigenetic age acceleration indicate that an individual is epigenetically older than would be expected given these covariates, whereas negative values for epigenetic age acceleration indicate that an individual is epigenetically younger than expected. The measure is (by definition) uncorrelated with

age. The distribution of epigenetic age acceleration within the sample is shown in Figure 1B, and the trait heritability estimate ($n = 628$, h$^2 = 0.374$, $p = 6.00 \times 10^{-7}$, SE = 0.097) is in line with previous findings (Horvath, 2013; Marioni et al., 2015a; Lu et al., 2016). The proportion of variance accounted for by covariates in this model was 0.864. We note that, in our sample, sex is not a significant covariate ($p = 0.305$) but is retained in the model nonetheless.

White matter integrity and chronological age

As has been previously shown, global white matter tract integrity was heritable in the sample (h$^2 = 0.506$, $p = 1.65 \times 10^{-5}$). There was no evidence of sex differences in white matter tract integrity (sex is not a significant covariate in the model, $p = 0.597$), but we did observe a strong age effect; age was a significant covariate in the heritability model ($p = 2.75 \times 10^{-13}$) and there was a significant negative phenotypic correlation between global white matter integrity and age (Fig. 2). For the specific white matter tracts, all were heritable and all, except the cingulum (hippocampus), showed a significant negative phenotypic correlation with age. Statistics are shown in Table 1.

Global white matter integrity and epigenetic age acceleration

Given that the integrity of white matter is correlated across the brain and the global measure of white matter integrity includes peripheral FA estimates not captured in specific tracts, we used the global measure as an omnibus test, before examining specific tract-based variation. The global index was negatively phenotypically correlated ($\rho_{\text{pheno}} = -0.119$, $p = 0.028$) with the blood-based epigenetic index of age acceleration, showing that individuals with blood samples that are epigenetically older than expected have reduced global FA in the brain. We decomposed this phenotypic correlation into genetic and environmental influences, finding evidence for common genetic ($\rho_{\text{gene}} = -0.460$, $p = 0.014$), but not environmental ($\rho_{\text{env}} = 0.222$, $p = 0.174$), factors. As the genetic correlation was negative, it suggests that the genes that increase epigenetic age acceleration in blood are also associated with reduced white matter integrity in brain.

Both diabetes and hypertension are age-linked traits that have been associated with changes in white matter tract integrity. We confirmed that the relationship between epigenetic age acceleration and global white matter tract integrity remained significant when covarying for either diabetes ($\rho_{\text{pheno}} = -0.112$, $p = 0.038$) or hypertension ($\rho_{\text{pheno}} = -0.116$, $p = 0.031$).

Specific tract-based white matter integrity and epigenetic age acceleration

To determine neuroanatomic specificity of this effect, we next examined FA in individual tracts. Seven of the 16 tracts were phenotypically correlated with epigenetic age acceleration where $p < 0.05$ (the anterior and posterior corona radiata, the genu, body and splenium of the corpus callosum, the posterior thalamic radiation, and the superior frontal-occipital fasciculus). Three of these (the posterior corona radiata and the body and splenium of the corpus callosum) remain significant when using an FDR correction of <0.05 across all 16 tracts. Results are shown in Table 1. In all cases, the phenotypic relationship between age acceleration and white matter integrity is negative, matching the direction of effects observed with the global white matter measure.

For the seven tracts where the phenotypic correlation with epigenetic age acceleration reached the nominal significance threshold of $p < 0.05$, we decomposed the correlations into genetic and environmental influences. Five tracts gave genetic

Figure 1. Epigenetic age measures. Top, Chronological age compared with epigenetic age estimates; correlation slope shown. Light gray represents females. Dark gray represents males. Bottom, Distribution of epigenetic age acceleration measure (i.e., epigenetic age covarying for age, sex, age $\times$ sex, age ^{2}, and age ^{2} $\times$ sex, and cell composition in blood). If values are $>$0 (to the right of the vertical line), this indicates individuals have epigenetic age estimates that are older than would be expected given the covariates; if values are $<$0, this indicates that epigenetic age estimates are younger than expected.

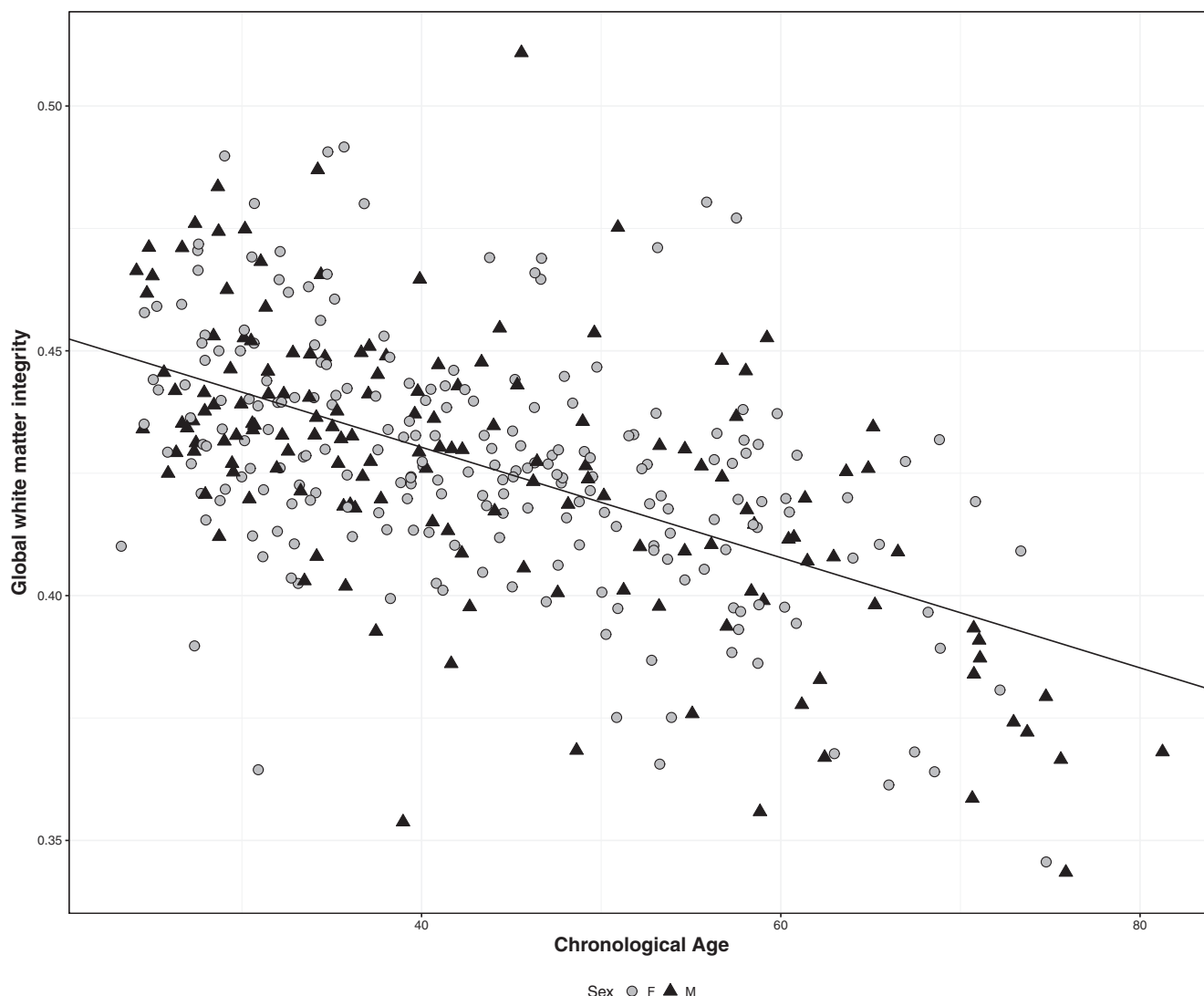**Figure 2.** Relationship between chronological age and global white matter integrity. Light gray represents females. Dark gray represents males.

correlations where $p < 0.05$ (i.e., all traits except the posterior thalamic radiation and superior frontal-occipital fasciculus). In each case, the genetic correlation was negative, as with the global FA measure.

Only the anterior corona radiata shows evidence of shared environmental influences with age acceleration ($\rho_{environ} = 0.428$, $p = 0.013$), but in this case the relationship is positive, indicating that environments that are linked to increased epigenetic age acceleration are also associated with increased white matter integrity in this tract.

White matter hyperintensity
There is evidence that white matter hyperintensity lesions may also track with age. However, in our sample, there was not a linear relationship with age across adulthood; instead, we observed that larger hyperintensity volumes only appear beyond the fifth decade of life (Fig. 3), in line with previous findings (Habes et al., 2016). Reflecting this, the phenotypic correlation with age, while still highly significant ($\rho_{pheno} = 0.426$, $p = 1.12 \times 10^{-15}$), is lower for white matter hyperintensity volume than for white matter integrity. Reflecting this weaker relationship with age across adulthood, the phenotypic correlation between white matter hy-

perintensity volume and epigenetic age acceleration is not significant ($\rho_{pheno} = 0.097$, $p = 0.063$).

Cell count estimates
In light of a previous study, which observed that both epigenetic age acceleration and granulocyte cell counts are related to Parkinson's disease (Horvath and Ritz, 2015), we undertook a secondary analysis examining the relationship between cell count estimates and our phenotypes of interest (Table 2).

Briefly, we find that the phenotypic correlations between cell counts and epigenetic age acceleration broadly reflect those seen with age in this sample. When considering cell counts in relation to global white matter tract integrity, the strongest phenotypic correlation that we see is with granulocyte count, which is negative in direction ($\rho_{pheno} = -0.170$, $p = 1.29 \times 10^{-3}$). The effect appears to be independent of any age- or epigenetic age acceleration-related effects.

Discussion
Both epigenetic age acceleration and white matter tract integrity traits are heritable in this sample, with estimates aligning closely with previous findings (Horvath, 2013; Jahanshad et al., 2013;

Table 1. White matter integrity measures and correlations with chronological age and epigenetic age acceleration[a]

	Heritability			Chronological age Phenotypic correlation			Epigenetic age acceleration Phenotypic correlation			Genetic correlation		Environmental correlation	
DTI trait	h^2	p	FDR	ρ	p	FDR	ρ	p	FDR	ρ	p	ρ	p
Global white-matter tract integrity	0.506*	1.65E-05*	NA	−0.542*	5.13E-32*	NA	−0.119*	0.028*	NA	−0.463*	0.013*	0.213	0.223
Corpus callosum (body)	0.502*	1.12E-05*	2.24E-05*	−0.464*	1.06E-22*	3.39E-22*	−0.167*	0.002*	0.011*	−0.571*	1.35E-03*	0.243	0.102
Corona radiata (posterior)	0.470*	6.70E-06*	1.53E-05*	−0.458*	6.94E-22*	1.23E-21*	−0.166*	0.002*	0.011*	−0.512*	4.67E-03*	0.153	0.307
Corpus callosum (splenium)	0.652*	2.00E-07*	1.60E-06*	−0.429*	4.91E-20*	7.86E-20*	−0.164*	0.002*	0.011*	−0.452*	7.21E-03*	0.219	0.279
Corona radiata (anterior)	0.563*	2.00E-06*	6.40E-06*	−0.505*	3.98E-27*	3.18E-26*	−0.118*	0.029*	0.091*	−0.588*	6.89E-04*	0.428*	0.013*
Corpus callosum (genu)	0.666*	4.00E-07*	2.13E-06*	−0.459*	2.61E-22*	6.13E-22*	−0.112*	0.037*	0.091*	−0.453*	7.32E-03*	0.375	0.072
Posterior thalamic radiation	0.450*	5.49E-05*	7.99E-05*	−0.502*	2.41E-26*	1.29E-25*	−0.114*	0.036*	0.091*	−0.329	0.107	0.009	0.703
Superior frontal-occipital fasciculus	0.521*	6.00E-07*	2.40E-06*	−0.393*	1.77E-15*	2.18E-15*	−0.109*	0.04*	0.091*	−0.333	0.072	0.086	0.561
Corona radiata (superior)	0.634*	1.00E-07*	1.60E-06*	−0.398*	1.38E-15*	1.84E-15*	−0.064	0.226	0.278	—	—	—	—
Sagittal stratum	0.378*	1.26E-03*	1.44E-03*	−0.464*	2.68E-22*	6.13E-22*	−0.091	0.097	0.162	—	—	—	—
Internal capsule (retrolenticular)	0.410*	6.61E-04*	8.14E-04*	−0.434*	5.74E-19*	8.35E-19*	−0.096	0.082	0.162	—	—	—	—
Internal capsule (anterior limb)	0.473*	3.90E-04*	5.20E-04*	−0.379*	8.31E-15*	9.50E-15*	−0.088	0.101	0.162	—	—	—	—
Cingulum (cingulate gyrus)	0.526*	1.45E-05*	2.58E-05*	−0.457*	3.25E-22*	6.50E-22*	−0.08	0.143	0.208	—	—	—	—
Cingulum (hippocampus)	0.374*	3.39E-03*	3.62E-03*	−0.058	0.270	0.270	−0.061	0.223	0.278	—	—	—	—
Superior longitudinal fasciculus	0.496*	2.87E-05*	4.59E-05*	−0.514*	7.09E-29*	1.13E-27*	−0.049	0.406	0.46	—	—	—	—
External capsule	0.583*	3.70E-06*	9.87E-06*	−0.544*	2.47E-25*	9.88E-25*	−0.048	0.431	0.46	—	—	—	—
Internal capsule (posterior limb)	0.331*	9.77E-03*	9.77E-03*	−0.308*	1.06E-09*	1.13E-09*	−0.022	0.63	0.63	—	—	—	—

[a]The primary outcome was global white matter tract integrity. Further investigation was then undertaken to look at the 16 specific DTI tracts available; an FDR threshold was applied across these 16 traits. Decomposition of phenotypic correlations with epigenetic age acceleration into genetic and environmental influences is shown for all traits where phenotypic correlations $p < 0.05$. No decomposition was undertaken for phenotypic correlations with chronological age as this is not heritable.

*$p < 0.05$.

Kochunov et al., 2015; Marioni et al., 2015a). We observe negative phenotypic correlations between these two traits both globally and within a number of specific white matter tracts in the brain. Decomposition of each of these phenotypic correlations reveals negative genetic correlations between epigenetic age acceleration and white matter integrity. Only one white matter tract (anterior corona radiata) showed significant (positive) environmental correlation with epigenetic age acceleration. Therefore, our results show that, when epigenetic age estimates in blood are older than would be expected, this is associated with reduced white matter tract integrity, and there are common genetic influences acting on both phenotypes.

While the relationship between age acceleration and tract integrity did not reach significance for a number specific white matter tracts tested, all showed the same pattern of negative phenotypic correlations with epigenetic age acceleration, suggesting that further examination in larger samples with greater statistical power would be of interest to establish whether the observed relationship with epigenetic age acceleration is global or focused in specific brain tracts.

In either case, these phenotypic and genetic correlations provide an interesting window into the neurobiology of aging processes within the brain. While the observed pleiotropic influences provide a causal genetic anchor linking epigenetic age acceleration with white matter integrity, evidence of genetic correlation is not sufficient to determine the processes that link these two traits, there are number of possible causal models that could be underlie this shared genetic etiology. Further work is necessary to determine the biological pathways linking these two processes and lead toward the delineation of the mechanisms involved in normal and pathological brain aging. Identification of the specific genes involved offers a useful starting point.

In terms of the biological meaning of the epigenetic age estimation, Horvath (2013) suggests that, as the measure seems to be distinct from cellular senescence and mitotic age, the epigenetic clock captures work done by an epigenetic maintenance system, which works to maintain epigenetic stability. Further work also shows that telomere length changes are also independent of changes in the epigenetic clock (Breitling et al., 2016; Lowe et al., 2016; Marioni et al., 2016).

Looking beyond cellular processes, epigenetic age acceleration has also been indicated as a biomarker for a number of other age-related traits; for example, among older individuals, relationships between accelerated epigenetic aging in blood and physical fitness, cognitive fitness, Parkinson's disease, and all-cause mortality have been reported (Horvath and Ritz, 2015; Marioni et al., 2015a, b; Chen et al., 2016). In samples that span adulthood, associations between epigenetic age acceleration in the blood and stress exposure and post-traumatic stress disorder have also been found (Boks et al., 2015; Zannas et al., 2015).

In this study, we also assess epigenetic aging in the blood with reference to brain-based traits. There have been several studies looking at different disorders linked to accelerated aging (including Huntingdon's disease, Down's syndrome, and HIV infection) that have shown the relationship to increased epigenetic aging can be seen in both blood and brain tissue samples (Horvath and Levine, 2015; Horvath et al., 2015a, 2016b). When multiple samples from the same individual have been available for comparison, there has been good consistency between epigenetic age estimates from different tissues, including blood and brain (Horvath, 2013; Horvath et al., 2015b). Additionally, evidence indicates that there is high convergence between epigenetic profiles in different tissues from the same individual, and correlations between blood and brain methylation levels are notably higher than those observed for gene expression (Horvath et al., 2012; Horvath, 2013).

Nevertheless, there are also examples of tissue-specific accelerated aging processes (Horvath et al., 2014). The phenotypic correlations reported here are modest; their magnitude is comparable with that previously reported between epigenetic age acceleration as mea-
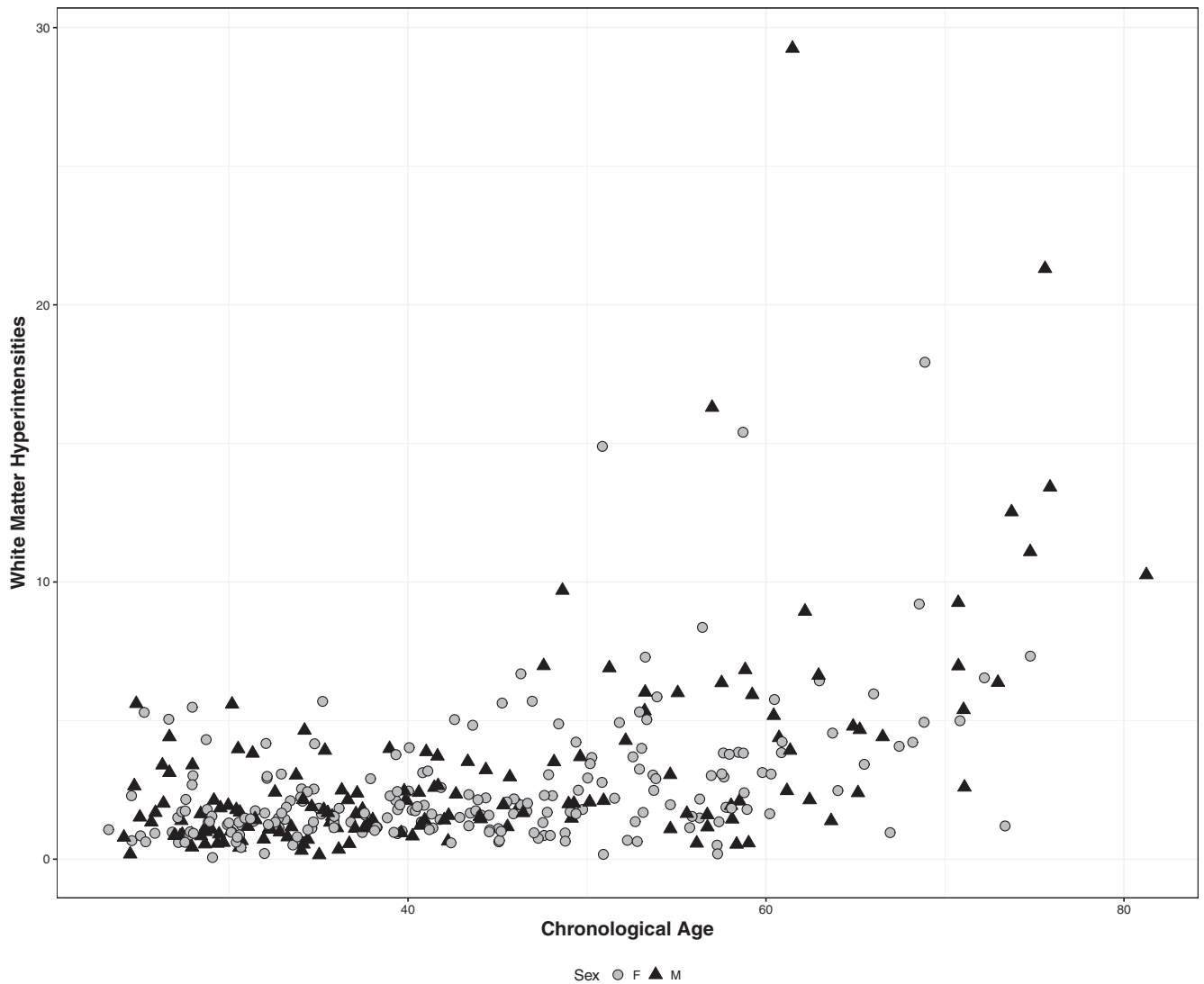
Figure 3. Relationship between chronological age and white matter hyperintensity volume. Light gray represents females. Dark gray represents males.

Table 2. Cell abundance estimations and correlations with traits of interest[a]

	Heritability			Chronological age			Epigenetic age acceleration							Global white-matter tract integrity						
				Phenotypic correlation			Phenotypic correlation			Genetic correlation		Environmental correlation		Phenotypic correlation			Genetic correlation		Environmental correlation	
Cell types	h²	p	FDR	ρ	p	FDR	ρ	p	FDR	ρ	p	ρ	p	ρ	p	FDR	ρ	p	ρ	p
Naive CD8 T	0.628*	5.45E-15*	1.91E-14*	−0.580*	4.43E-67*	3.10E-66*	−0.146*	9.17E-04*	2.14E-03*	0.010	0.950	−0.312*	0.014*	0.091	0.111	0.155	—	—	—	—
CD4 T	0.359*	2.80E-06*	2.80E-06*	−0.117*	3.27E-03*	5.72E-03*	−0.164*	1.05E-04*	7.35E-04*	−0.059	0.780	−0.219*	0.029*	0.105*	0.043*	0.086*	0.135	0.521	0.085	0.565
Granulocytes	0.519*	1.61E-11*	2.82E-11*	0.015	0.712	0.712	0.010	0.814	0.814	—	—	—	—	−0.170*	1.29E-03*	9.03E-03*	−0.292	0.125	−0.049	0.758
Monocytes	0.394*	6.00E-07*	7.00E-07*	0.072	0.072	0.101	0.046	0.274	0.320	—	—	—	—	−0.024	0.658	0.658	—	—	—	—
Natural killer	0.656*	3.27E-24*	2.29E-23*	0.342*	1.49E-23*	5.22E-23*	0.053	0.214	0.300	—	—	—	—	0.116*	0.026*	0.086*	0.214	0.160	−0.010	0.952
Plasmablast	0.512*	1.97E-12*	4.60E-12*	0.016	0.683	0.712	0.066	0.124	0.217	—	—	—	—	−0.108*	0.049*	0.086*	−0.264	0.168	0.044	0.780
CD8 + CD28-CD45RA-T	0.410*	1.00E-07*	1.40E-07*	0.306*	9.06E-15*	2.11E-14*	0.149*	4.02E-04*	1.41E-03*	0.193	0.339	0.125	0.206	−0.045	0.398	0.464	—	—	—	—

[a]An FDR correction was applied across the 7 cell types considered. Phenotypic correlations between cell abundances and epigenetic age acceleration or global white matter tract integrity were decomposed into genetic and environmental influences when phenotypic correlations $p < 0.05$. No decomposition was undertaken for phenotypic correlations with chronological age as this is not heritable.

*$p < 0.05$.

sured in dorsolateral prefrontal cortex tissue and neuropathological measures associated with Alzheimer's disease (Levine et al., 2015). Given examples of tissue-specific accelerated aging, it could be speculated that stronger associations between epigenetic age acceleration and white matter integrity might be observed if age acceleration was measured using brain tissue rather than blood. However, there is a distinct advantage in being able to use an easily accessible tissue, such as blood, for this potential biomarker of healthy and pathological brain aging, including that the biomarker can be assessed at multiple points throughout the lifespan.

The evidence to date suggests that, although there may be some pathological processes leading to tissue-specific age acceleration, in general blood can serve as a useful surrogate tissue for the development of aging biomarkers, particularly when the most relevant tissue is not easily accessible, as is the case when looking at brain traits.

We also performed a secondary analysis examining cell count estimates in the blood and how these relate to both age and white matter integrity. We find a negative correlation between granulocytes and white matter integrity that is independent of age-related effects. This pattern of results echoes the relationship observed previously in Parkinson's disease using similar methods, whereby patients were observed to not only show increased epigenetic accelerated aging but also have more granulocytes than controls (Horvath and Ritz, 2015). Although we are unable to distinguish between granulocyte subtypes, given that neutrophils are far more prevalent than eosinophils or basophils (accounting for 60%–70%, 2%–4%, and 0.5%–1% of white blood cells, respectively), it is likely that they are driving the observed association. But clearly, further work is needed to understand this relationship with white matter integrity. As we are using indirectly estimating relative cell abundance measures from epigenetic data, replication with direct measurements of cell types is also needed.

In conclusion, acceleration in epigenetic aging shows negative phenotypic and genetic correlations with white matter integrity both globally and within a number of specific tracts within the brain. This suggests that the epigenetic clock may prove a useful biomarker of normal and pathological brain aging across the adult lifespan. The shared genetic influences on these two traits offer a method by which researchers can begin to unpick the neurobiological processes underpinning variation in age-related changes in the brain.

References

Benjamini Y, Hochberg Y (1995) Controlling the false discovery rate: a practical and powerful approach to multiple testing. J R Stat Soc Ser B 57:289–300.

Bishop NA, Lu T, Yankner BA (2010) Neural mechanisms of ageing and cognitive decline. Nature 464:529–535. CrossRef Medline

Boks MP, van Mierlo HC, Rutten BP, Radstake TR, De Witte L, Geuze E, Horvath S, Schalkwyk LC, Vinkers CH, Broen JC. Vermetten E (2015) Longitudinal changes of telomere length and epigenetic age related to traumatic stress and post-traumatic stress disorder. Psychoneuroendocrinology 51:506–512. CrossRef Medline

Breitling LP, Saum KU, Perna L, Schöttker B, Holleczek B, Brenner H (2016) Frailty is associated with the epigenetic clock but not with telomere length in a German cohort. Clin Epigenetics 8:21. CrossRef Medline

Chen BH, Marioni RE, Colicino E, Peters, MJ, Ward-Caviness CK, Tsai PC, Roetker NS, Just AC, Demerath EW, Guan W, Bressler J, Fornage M, Studenski S, Vandiver AR, Moore AZ, Tanaka T, Kiel DP, Liang L, Volkonas P, Schwartz J, et al (2016) DNA methylation-based measures of biological age: meta-analysis predicting time to death. Aging (Albany, NY) 8:1844–1865. CrossRef Medline

Cox SR, Ritchie SJ, Tucker-Drob EM, Liewald DC, Hagenaars SP, Davies G, Wardlaw JM, Gale CR, Bastin ME, Deary IJ (2016) Ageing and brain white matter structure in 3,513 UK Biobank participants. Nat Commun 7:13629. CrossRef Medline

Fraga MF, Ballestar E, Paz MF, Ropero S, Setien F, Ballestar ML, Heine-Suñer D, Cigudosa JC, Urioste M, Benitez J, Boix-Chornet M, Sanchez-Aguilera A, Ling C, Carlsson E, Poulsen P, Vaag A, Stephan Z, Spector TD, Wu YZ, Plass C, et al (2005) Epigenetic differences arise during the lifetime of monozygotic twins. Proc Natl Acad Sci U S A 102:10604–10609. CrossRef Medline

Giorgio A, Santelli L, Tomassini V, Bosnell R, Smith S, De Stefano N, Johansen-Berg H (2010) Age-related changes in grey and white matter structure throughout adulthood. Neuroimage 51:943–951. CrossRef Medline

Glahn DC, Kent JW Jr, Sprooten E, Diego VP, Winkler AM, Curran JE, McKay DR, Knowles EE, Carless MA, Göring HH, Dyer TD, Olvera RL, Fox PT, Almasy L, Charlesworth J, Kochunov P, Duggirala R, Blangero J (2013) Genetic basis of neurocognitive decline and reduced white matter integrity in normal human brain aging. Proc Natl Acad Sci U S A 110:19006–19011. CrossRef Medline

Habes M, Erus G, Toledo JB, Zhang T, Bryan N, Launer LJ, Rosseel Y, Janowitz D, Doshi J, Van der Auwera S, von Sarnowski B, Hegenscheid K, Hosten N, Homuth G, Völzke H, Schminke U, Hoffmann W, Grabe HJ, Davatzikos C (2016) White matter hyperintensities and imaging patterns of brain ageing in the general population. Brain 139:1164–1179. CrossRef Medline

Hannum G, Guinney J, Zhao L, Zhang L, Hughes G, Sadda S, Klotzle B, Bibikova M, Fan JB, Gao Y, Deconde R, Chen M, Rajapakse I, Friend S, Ideker T, Zhang K (2013) Genome-wide methylation profiles reveal quantitative views of human aging rates. Mol Cell 49:359–367. CrossRef Medline

Horvath S (2013) DNA methylation age of human tissues and cell types. Genome Biol 14:R115. CrossRef Medline

Horvath S, Gurven M, Levine ME, Trumble BC, Kaplan H, Allayee H, Ritz BR, Chen B, Lu AT, Rickabaugh TM, Jamieson BD, Sun D, Li S, Chen W, Quintana-Murci L, Fagny M, Kobor MS, Tsao PS, Reiner AP, Edlefsen KL, et al (2016a) An epigenetic clock analysis of race/ethnicity, sex, and coronary heart disease. Genome Biol 17:171. CrossRef Medline

Horvath S, Levine AJ (2015) HIV-1 infection accelerates age according to the epigenetic clock. J Infect Dis 212:1563–1573. CrossRef Medline

Horvath S, Ritz BR (2015) Increased epigenetic age and granulocyte counts in the blood of Parkinson's disease patients. Aging (Albany, NY) 7:1130–1142. CrossRef Medline

Horvath S, Zhang Y, Langfelder P, Kahn RS, Boks MP, van Eijk K, van den Berg LH, Ophoff RA (2012) Aging effects on DNA methylation modules in human brain and blood tissue. Genome Biol 13:R97. CrossRef Medline

Horvath S, Erhart W, Brosch M, Ammerpohl O, von Schönfels W, Ahrens M, Heits N, Bell JT, Tsai PC, Spector TD, Deloukas P, Siebert R, Sipos B, Becker T, Röcken C, Schafmayer C, Hampe J (2014) Obesity accelerates epigenetic aging of human liver. Proc Natl Acad Sci U S A 111:15538–15543. CrossRef Medline

Horvath S, Garagnani P, Bacalini MG, Pirazzini C, Salvioli S, Gentilini D, Di Blasio AM, Giuliani C, Tung S, Vinters HV, Franceschi C (2015a) Accelerated epigenetic aging in Down syndrome. Aging Cell 14:491–495. CrossRef Medline

Horvath S, Mah V, Lu AT, Woo JS, Choi OW, Jasinska AJ, Riancho JA, Tung S, Coles NS, Braun J, Vinters HV, Coles LS (2015b) The cerebellum ages slowly according to the epigenetic clock. Aging (Albany NY) 7:294–306. CrossRef Medline

Horvath S, Langfelder P, Kwak S, Aaronson J, Rosinski J, Vogt TF, Eszes M, Faull RL, Curtis MA, Waldvogel HJ, Choi OW, Tung S, Vinters HV, Coppola G, Yang XW (2016b) Huntington's disease accelerates epigenetic aging of human brain and disrupts DNA methylation levels. Aging (Albany NY) 8:1485–1512. CrossRef Medline

Houseman EA, Accomando WP, Koestler DC, Christensen BC, Marsit CJ, Nelson HH, Wiencke JK, Kelsey KT (2012) DNA methylation arrays as surrogate measures of cell mixture distribution. BMC Bioinformatics 13:86. CrossRef Medline

Jahanshad N, Kochunov PV, Sprooten E, Mandl RC, Nichols TE, Almasy L, Blangero J, Brouwer RM, Curran JE, de Zubicaray GI, Duggirala R, Fox PT, Hong LE, Landman BA, Martin NG, McMahon KL, Medland SE, Mitchell BD, Olvera RL, Peterson CP, et al (2013) Multi-site genetic analysis of diffusion images and voxelwise heritability analysis: a pilot project of the ENIGMA-DTI working group. Neuroimage 81:455–469. CrossRef Medline

Jones MJ, Goodman SJ, Kobor MS (2015) DNA methylation and healthy human aging. Aging Cell 14:924–932. CrossRef Medline

Kochunov P, Jahanshad N, Marcus D, Winkler A, Sprooten E, Nichols TE, Wright SN, Hong LE, Patel B, Behrens T, Jbabdi S, Andersson J, Lenglet C, Yacoub E, Moeller S, Auerbach E, Ugurbil K, Sotiropoulos SN, Brouwer RM, Landman B, et al (2015) Heritability of fractional anisotropy in human white matter: a comparison of Human Connectome Project and ENIGMA-DTI data. Neuroimage 111:300–311. CrossRef Medline

Kochunov P, Glahn D, Lancaster J, Winkler A, Kent JW Jr, Olvera RL, Cole

SA, Dyer TD, Almasy L, Duggirala R, Fox PT, Blangero J (2010) Whole brain and regional hyperintense white matter volume and blood pressure: overlap of genetic loci produced by bivariate, whole-genome linkage analyses. Stroke 41:2137–2142. CrossRef Medline

Kulkarni H, Kos MZ, Neary J, Dyer TD, Kent JW Jr, Göring HH, Cole SA, Comuzzie AG, Almasy L, Mahaney MC, Curran JE, Blangero J, Carless MA (2015) Novel epigenetic determinants of type 2 diabetes in Mexican-American families. Hum Mol Genet 24:5330–5344. CrossRef Medline

Levine ME, Lu AT, Bennett DA, Horvath S (2015) Epigenetic age of the pre-frontal cortex is associated with neuritic plaques, amyloid load, and Alzheimer's disease related cognitive functioning. Aging (Albany NY) 7:1198–1211. CrossRef Medline

Lowe D, Horvath S, Raj K (2016) Epigenetic clock analyses of cellular senescence and ageing. Oncotarget 7:8524–8531. CrossRef Medline

Lu AT, Hannon E, Levine ME, Hao K, Crimmins EM, Lunnon K, Kozlenkov A, Mill J, Dracheva S, Horvath S (2016) Genetic variants near MLST8 and DHX57 affect the epigenetic age of the cerebellum. Nat Commun 7:10561. CrossRef Medline

Marioni RE, Shah S, McRae AF, Chen BH, Colicino E, Harris SE, Gibson J, Henders AK, Redmond P, Cox SR, Pattie A, Corley J, Murphy L, Martin NG, Montgomery GW, Feinberg AP, Fallin MD, Multhaup ML, Jaffe AE, Joehanes R, et al (2015a) DNA methylation age of blood predicts all-cause mortality in later life. Genome Biol 16:25. CrossRef Medline

Marioni RE, Shah S, McRae AF, Ritchie SJ, Muniz-Terrera G, Harris SE, Gibson J, Redmond P, Cox SR, Pattie A, Corley J, Taylor A, Murphy L, Starr JM, Horvath S, Visscher PM, Wray NR, Deary IJ (2015b) The epigenetic clock is correlated with physical and cognitive fitness in the Lothian Birth Cohort 1936. Int J Epidemiol 44:1388–1396. CrossRef Medline

Marioni RE, Harris SE, Shah S, McRae AF, von Zglinicki T, Martin-Ruiz C, Wray NR, Visscher PM, Deary IJ (2016) The epigenetic clock and telomere length are independently associated with chronological age and mortality. Int J Epidemiol. Advance online publication. Retrieved Apr. 13, 2016. doi: 10.1093/ije/dyw041. CrossRef Medline

Mather M, Jacobsen LA, Pollard KM (2015) Aging in the United States. Popul Bull 70.

Mitchell BD, Kammerer CM, Blangero J, Mahaney MC, Rainwater DL, Dyke B, Hixson JE, Henkel RD, Sharp RM, Comuzzie AG, VandeBerg JL, Stern MP, MacCluer JW (1996) Genetic and environmental contributions to cardiovascular risk factors in Mexican-Americans: the San Antonio Family Heart Study. Circulation 94:2159–2170. CrossRef Medline

Mori S, Oishi K, Jiang H, Jiang L, Li X, Akhter K, Hua K, Faria AV, Mahmood A, Woods R, Toga AW, Pike GB, Neto PR, Evans A, Zhang J, Huang H, Miller MI, van Zijl P, Mazziotta J (2008) Stereotaxic white matter atlas based on diffusion tensor imaging in an ICBM template. Neuroimage 40:570–582. CrossRef Medline

Moseley M (2002) Diffusion tensor imaging and aging: a review. NMR Biomed 15:553–560. CrossRef Medline

Olvera RL, Bearden CE, Velligan DI, Almasy L, Carless MA, Curran JE, Williamson DE, Duggirala R, Blangero J, Glahn DC (2011) Common genetic influences on depression, alcohol, and substance use disorders in Mexican-American families. Am J Med Genet B Neuropsychiatr Genet 156B:561–568. CrossRef Medline

Puppala S, Dodd GD, Fowler S, Arya R, Schneider J, Farook VS, Granato R, Dyer TD, Almasy L, Jenkinson CP, Diehl AK, Stern MP, Blangero J, Duggirala R (2006) A genomewide search finds major susceptibility loci for gallbladder disease on chromosome 1 in Mexican-Americans. Am J Hum Genet 78:377–392. CrossRef Medline

Smith SM, Jenkinson M, Johansen-Berg H, Rueckert D, Nichols TE, Mackay CE, Watkins KE, Ciccarelli O, Cader MZ, Matthews PM, Behrens TE (2006) Tract-based spatial statistics: voxelwise analysis of multi-subject diffusion data. Neuroimage 31:1487–1505. CrossRef Medline

Sprooten E, Knowles EE, McKay DR, Göring HH, Curran JE, Kent JW, Carless MA, Dyer TD, Drigalenko EI, Olvera RL, Fox PT, Almasy L, Duggirala R, Kochunov P, Blangero J, Glahn DC (2014) Common genetic variants and gene expression associated with white matter microstructure in the human brain. Neuroimage 97:252–261. CrossRef Medline

Sullivan EV, Pfefferbaum A (2006) Diffusion tensor imaging and aging. Neurosci Biobehav Rev 30:749–761. CrossRef Medline

Teipel SJ, Meindl T, Wagner M, Stieltjes B, Reuter S, Hauenstein KH, Filippi M, Ernemann U, Reiser MF, Hampel H (2010) Longitudinal changes in fiber tract integrity in healthy aging and mild cognitive impairment: a DTI follow-up study. J Alzheimers Dis 22:507–522. CrossRef Medline

Teschendorff AE, West J, Beck S (2013) Age-associated epigenetic drift: implications, and a case of epigenetic thrift? Hum Mol Genet 22:R7–R15. CrossRef Medline

United Nations Department of Economic and Social Affairs Population Division (2015) World Population Ageing 2015. New York: United Nations.

van Boxtel MP, Buntinx F, Houx PJ, Metsemakers JF, Knottnerus A, Jolles J (1998) The relation between morbidity and cognitive performance in a normal aging population. J Gerontol A Biol Sci Med Sci 53:M147–M154. Medline

Weidner CI, Lin Q, Koch CM, Eisele L, Beier F, Ziegler P, Bauerschlag DO, Jöckel KH, Erbel R, Mühleisen TW, Zenke M, Brümmendorf TH, Wagner W (2014) Aging of blood can be tracked by DNA methylation changes at just three CpG sites. Genome Biol 15:R24. CrossRef Medline

Zannas AS, Arloth J, Carrillo-Roa T, Iurato S, Röh S, Ressler KJ, Nemeroff CB, Smith AK, Bradley B, Heim C, Menke A, Lange JF, Brückl T, Ising M, Wray NR, Erhardt A, Binder EB, Mehta D (2015) Lifetime stress accelerates epigenetic aging in an urban, African American cohort: relevance of glucocorticoid signaling. Genome Biol 16:266. CrossRef Medline